Title

A role for the fornix in temporal sequence memory

Journal

European Journal of Neuroscience, 57(7)

ISSN

0953-816X

Authors

Read, Marie-Lucie

Umla-Runge, Katja

Lawrence, Andrew D

et al.

Publication Date

2023-04-01

DOI

10.1111/ejn.15940

Received: 1 August 2022 | Revised: 31 January 2023 | Accepted: 15 February 2023

DOI: 10.1111/ejn.15940

RESEARCH REPORT

EJN European Journal of Neuroscience FENS WILEY

A role for the fornix in temporal sequence memory

Marie-Lucie Read[1] | **Katja Umla-Runge**[2] | **Andrew D. Lawrence**[1] | **Alison G. Costigan**[1] | **Liang-Tien Hsieh**[3] | **Maxime Chamberland**[1,4] | **Charan Ranganath**[5] | **Kim S. Graham**[1]

[1]Cardiff University Brain Research Imaging Centre (CUBRIC), School of Psychology, Cardiff University, Cardiff, UK

[2]School of Medicine, Cardiff University, Cardiff, UK

[3]Helen Willis Neuroscience Institute, University of California, Berkeley, Berkeley, California, USA

[4]Department of Mathematics and Computer Science, Eindhoven University of Technology, Eindhoven, Netherlands

[5]Center for Neuroscience, Department of Psychology, University of California, Davis, Davis, California, USA

Correspondence
Marie-Lucie Read, Cardiff University Brain Research Imaging Centre (CUBRIC), School of Psychology, Cardiff University, Cardiff, UK.
Email: readms2@cardiff.ac.uk

Present address
Kim S. Graham, Department of Psychology, University of Edinburgh, Edinburgh, UK.

Funding information
This work was supported by a Wellcome Strategic Award (Wellcome Trust, 104943/Z/14/Z) to K.G.; a Wellcome Institutional Strategic Support Fund award to A.D.L.; a departmental PhD studentship from the School of Psychology, Cardiff University, to M.-L.R.; a Biotechnology and Biological Sciences Research Council Award to A.D.L. and K.G. (BB/V008242/1); and a Vannevar Bush Faculty Fellowship (Office of Naval Research Grant

Abstract

Converging evidence from studies of human and nonhuman animals suggests that the hippocampus contributes to sequence learning by using temporal context to bind sequentially occurring items. The fornix is a white matter pathway containing the major input and output pathways of the hippocampus, including projections from medial septum and to diencephalon, striatum, lateral septum and prefrontal cortex. If the fornix meaningfully contributes to hippocampal function, then individual differences in fornix microstructure might predict sequence memory. Here, we tested this prediction by performing tractography in 51 healthy adults who had undertaken a sequence memory task. Microstructure properties of the fornix were compared with those of tracts connecting medial temporal lobe regions but not predominantly the hippocampus: the Parahippocampal Cingulum bundle (PHC) (conveying retrosplenial projections to parahippocampal cortex) and the Inferior Longitudinal Fasciculus (ILF) (conveying occipital projections to perirhinal cortex). Using principal components analysis, we combined Free-Water Elimination Diffusion Tensor Imaging and Neurite Orientation Dispersion and Density Imaging measures obtained from

List of abbreviations: AD, axial diffusivity; BF, Bayes factor; dMRI, diffusion-weighted Magnetic Resonance Imaging; DTI, diffusion tensor Imaging; DWI, diffusion-weighted Imaging; FA, fractional anisotropy; fMRI, functional Magnetic Resonance Imaging; fODF, fibre Orientation Density Function; FOV, field of view; FWE, free water elimination; FWE-AD, Axial Diffusivity (Free Water Elimination); FWE-DTI, Diffusion Tensor Imaging (with Free Water Elimination); FWE-FA, Fractional Anisotropy (Free Water Elimination); FWE-MD, Mean Diffusivity (Free Water Elimination); FWE-RD, Radial Diffusivity (Free Water Elimination); HARDI, High Angular Resolution Diffusion-Weighted Imaging; ILF, inferior longitudinal fasciculus; MD, mean diffusivity; MTL, medial temporal lobe; NDI, Neurite Density Index; NODDI, Neurite Orientation Dispersion and Density Imaging; ODI, Orientation Dispersion Index; PC, principal component; PCA, principal component analyses; PHC, Parahippocampal Cingulum Bundle; RD, radial diffusivity; RT, reaction time; TE, echo time; TR, repetition time.

Marie-Lucie Read and Katja Umla-Runge are co-first authors.

N00014-15-1-0033) to C.R. (any opinions, findings and conclusions or recommendations expressed in this material are those of the authors and do not necessarily reflect the views of the Office of Naval Research or the US Department of Defense).

Edited by: John Foxe

multi-shell diffusion MRI into two informative indices: the first (PC1) capturing axonal packing/myelin and the second (PC2) capturing microstructural complexity. We found a significant correlation between fornix PC2 and implicit reaction-time indices of sequence memory, indicating that greater fornix microstructural complexity is associated with better sequence memory. No such relationship was found with measures from the PHC and ILF. This study highlights the importance of the fornix in aiding memory for objects within a temporal context, potentially reflecting a role in mediating inter-regional communication within an extended hippocampal system.

KEYWORDS
diffusion MRI, episodic memory, fornix, hippocampus, sequence, time

1 | INTRODUCTION

The hippocampus is widely known to make a critical contribution to episodic memory. Considerable evidence suggests that the key contribution of the hippocampus might be to build memories that associate different pieces of information occuring in a shared spatiotemporal context (Aggleton & Brown, 2005; Eichenbaum, 2017; Ekstrom & Ranganath, 2018; Hsieh et al., 2014; Long & Kahana, 2019; Opitz, 2014). For instance, hippocampal lesions in animals disrupt memory for temporal order relationships (Eichenbaum, 2017; Heuer & Bachevalier, 2013; Ranganath & Hsieh, 2016). Furthermore, hippocampal neural activity patterns, measured with functional magnetic resonance imaging (fMRI), carry information about the temporal context of items in learned sequences (Hsieh et al., 2014; Kalm et al., 2013; Schapiro et al., 2012; Williams et al., 2023; for review, see Lee et al., 2020).

In particular, work by Hsieh et al. (2014) evidenced that the hippocampus uniquely carries information about the temporal order of objects in sequences, whereas other medial temporal lobe (MTL) regions, the perirhinal cortex and parahippocampal cortex, carry information about isolated object and temporal context information, respectively. Additionally, individual differences in sequence memory (indexed by the reaction time, RT, facilitation for semantic decisions on objects within consistently ordered sequences vs. randomly ordered sequences) strongly correlated with individual differences in hippocampal object-position binding bilaterally (indexed as the multi-voxel pattern similarity difference between hippocampal patterns during repetitions of the same item in consistent sequences and hippocampal patterns during repetitions of the same item in random sequences). The results indicate that the hippocampus has representational specializations that support sequence memory (Davachi & DuBrow, 2015).

However, it is clear that episodic memory relies not only on the hippocampus but also on a broader network of areas, so we aimed to elucidate how structural connectivity of the hippocampus with these broader areas relates to sequence memory. According to one hypothesis, episodic memory is supported by an 'extended hippocampal system', comprising the hippocampus, anterior thalamic nucleus, mamillary bodies and medial prefrontal cortex (Aggleton, 2012; Aggleton & Brown, 1999; Gaffan, 1992; Gaffan & Hornak, 1997). Murray et al. (2017, 2018) proposed that the prominence of integrated spatiotemporal representations in the primate extended hippocampal system reflects an inheritance from oligocene anthropoids, where background scenes supported foraging choices at a distance, an ability that was enhanced over evolution, enabling hippocampal representations to support spatio-temporal attributes of episodic memory in humans (Murray et al., 2017). Regions in the extended hippocampal system are inter-connected via the fornix, the main white matter tract entering and exiting the hippocampus (Aggleton, 2012; Aggleton & Brown, 1999; Bubb et al., 2017; Gaffan, 1992; Gaffan & Hornak, 1997). Thus, the fornix may play a critical role in bringing together elements of the extended hippocampal system in the service of episodic memory. Individual differences in microstructure of the fornix should therefore be associated with inter-individual variation in memory for objects in spatial and/or temporal context.

Indeed, human studies using diffusion-weighted Magnetic Resonance Imaging (dMRI), which can non-invasively delineate the path of major fibre pathways and evaluate their microstructure through indices such as Fractional Anisotropy (FA) (Assaf et al., 2019), have found that inter-individual differences in fornix microstructure in healthy individuals correlate with individual variation in spatial memory and scene discrimination performance (Bourbon-Teles et al., 2021; Hodgetts

et al., 2015; Hodgetts et al., 2017; Postans et al., 2014; Rudebeck et al., 2009; for review, see Benear et al., 2020). However, it is unclear whether fornix microstructure would similarly relate to temporal memory. While lesions of the fornix in macaque monkeys are known to impair choices based on relative recency (Charles et al., 2004), the contribution of the fornix to temporal sequence memory has not been investigated in healthy humans.

We investigated fornix contributions to memory for objects in temporal context, in healthy humans, using an adaptation of the sequence memory task of Hsieh et al. (2014). As in that study individual differences in the time taken to answer semantic questions about learned objects in consistently ordered sequences versus randomly ordered sequences (RT random - RT consistent) was used as an indirect measure of sequence memory (referred to as 'Sequence Memory Performance'). Larger Sequence Memory Performance scores would equate to a faster RT for consistently ordered sequences than for randomly ordered sequences, indicating that memory-based predictions (formed through repeated exposures to temporal regularities) (Davachi & DuBrow, 2015; Lisman & Redish, 2009) about upcoming objects in the predictable, relative to the unpredictable sequence, had aided performance (see also Williams et al., 2023)[1]. It was hypothesized that individual differences in fornix microstructure would relate to Sequence Memory Performance.

In contrast, we investigated the roles of the Parahippocampal Cingulum bundle (PHC) and Inferior Longitudinal Fasciculus (ILF), specifically with the expectation that these would not contribute to binding of objects within temporal sequences. The PHC connects the posterior cingulate and retrosplenial cortex with the parahippocampal cortex (Bubb et al., 2017, 2018), an area previously shown to hold temporal context information about sequences, but not conjoined object and temporal position information (Hsieh et al., 2014). The ILF is a major white matter tract in the ventral object processing stream, connecting occipital cortex with ventro-anterior temporal lobe, including the perirhinal cortex (Catani et al., 2003; Hodgetts et al., 2015), an area previously shown to hold object information regardless of any temporal sequence associations, but not conjoined object and temporal position information (Hsieh et al., 2014; see also Gaffan & Parker, 1996; Parker & Gaffan, 1997, for related evidence of a unique role for the hippocampus-fornix system, but not perirhinal or cingulate cortices, in the integration of objects and their position in space).

A multi-shell diffusion MRI protocol was applied allowing the combination of Free-Water Elimination Diffusion Tensor Imaging (FWE-DTI) and Neurite Orientation Dispersion and Density Imaging (NODDI) models to assess tract microstructural properties. While DTI has been successfully applied to study inter-individual differences in cognition and tract microstructure in healthy adults (e.g., Coad et al., 2020; Hodgetts et al., 2015, 2017; Postans et al., 2014), DTI measures lack biological specificity (Tournier et al., 2011). One way to increase specificity is to correct DTI measures for partial volume effects with extracellular water. Free-water elimination DTI (FWE-DTI) (Pasternak et al., 2009) adds a second compartment to the DTI model that explicitly accounts for the signal contribution of extracellular free water, such as cerebrospinal fluid. As a result, the DTI parameters (FA, MD, AD and RD) obtained through FWE-DTI are corrected for partial volume effects and thus better represent tissue microstructure. Furthermore, both axon density and fibre dispersion can influence FA (Beaulieu, 2002). The three-compartment model, NODDI, provides metrics sensitive to axon density, Neurite Density Index (NDI), and the extent of orientational dispersion within a voxel, Orientation Dispersion Index (ODI) (Zhang et al., 2012) in addition to an extracellular free-water compartment.

Although individual diffusion measures are related to somewhat different aspects of white matter microstructure, they also share information (Bells et al., 2011; de Santis et al., 2014). A dimensionality reduction framework, based on Principal Components Analysis (PCA), can take advantage of such redundancies to combine diffusion measures into more biologically informative measures of white matter microstructure (Chamberland et al., 2019; Geeraert et al., 2020). By adopting this novel approach, we were able to combine dMRI measures into meaningful indices of white matter microstructure and successfully examine the relationships between white matter microstructure of the fornix, ILF and PHC, and individual differences in sequence memory. Based on Hsieh et al. (2014), we predicted significant correlations between Sequence Memory Performance and fornix microstructure properties, but not between Sequence Memory Performance and ILF or PHC microstructure properties.

2 | MATERIALS AND METHODS

2.1 | Participants

Fifty-one female volunteers (mean age: 20.1 years, SD 1.1, range: 19–24 years) were recruited from the Cardiff

[1]Note that previous work referred to this measure as "RT Enhancement" (Hsieh et al., 2014; Random RT minus learned [consistently ordered, including overlapping sequence pairs] RT) or "sequence prediction effect" (Williams et al., 2023; Fixed [consistently ordered]-Random RT for objects 2-5).

University School of Psychology participant panel (a subsample of those described in Karahan et al., 2019). The study was approved by Cardiff University's School of Psychology Research Ethics Committee, and all volunteers gave informed consent prior to participation. Participants underwent behavioural testing followed by a diffusion MRI scan, within a 6-month period.

2.2 | Task procedures

The sequence memory task, adapted from Hsieh et al. (2014), comprised two sessions: a *learning session* and immediately followed by a *retrieval session*. In these, participants were asked to make semantic decisions about objects, including man-made objects, animals, fruits, and vegetables, that were presented in sequences of five objects. Participants answered different semantic questions in each of the two sessions, to ensure their responses were modulated by their memory of the temporal-sequential relationships among the objects, rather than learning at the level of motor responses or of object-response associations. Both sessions included consistently ordered (henceforth, *consistent*) and randomly ordered (henceforth, *random*) sequence types. Consistent sequences contained the same objects that always appeared in a fixed (and hence predictable) order: one of these sequences contained unique objects and another two sequences shared identical objects in serial positions 2 and 3 (but note that this is treated as one condition as in Crivelli-Decker et al., 2018). Two random sequences contained unique objects, but these were presented in a different order in every repetition. The retrieval session additionally included novel sequences, which contained novel and trial-unique objects upon every repetition (note: Response RTs to novel objects is not included in this study). Examples of the sequences are shown in Figure 1.

2.2.1 | Learning session

The learning session included two study-test cycles. In each *study cycle*, the three consistent and the two random sequences were each presented three times. One of five semantic yes/no questions, for example, 'Is the presented item readily edible?', was presented at the beginning of each cycle, and participants answered this question for each object presented within the cycle. Participants were instructed to answer as quickly and accurately as possible. The order of sequences was semi-randomized to ensure that sequences of the same type were not presented consecutively and that all sequences had been presented before showing repeats. Each object was displayed for 1 s and was followed by a blank fixation screen lasting 1.5 s. Participants could respond any time between object onset and the end of this fixation screen. The sequences were separated by a longer blank fixation screen lasting 2.5 s (see Figure 2 for more detail).

In each of the *test cycles* in the learning session, participants were shown all classes of sequences again. As above, the order of sequences was semi-randomized. Participants were explicitly tested on how well they had learned each of the consistent sequences, three times. They were shown all the objects from a sequence simultaneously, and these were labelled 1 to 5, with five boxes underneath each of the numbers. Participants were asked to reconstruct the order in which they were presented in that sequence, using keys 1 to 5 along the top of the keyboard. The correct order was then displayed. For the random sequence trials, participants simply placed the objects in a random order, and then, another random order was displayed, which required no response. There were two study-test cycles within the learning session. For consistent sequences, answers were scored correct if objects were placed in the correct temporal position. The fraction of answers that were

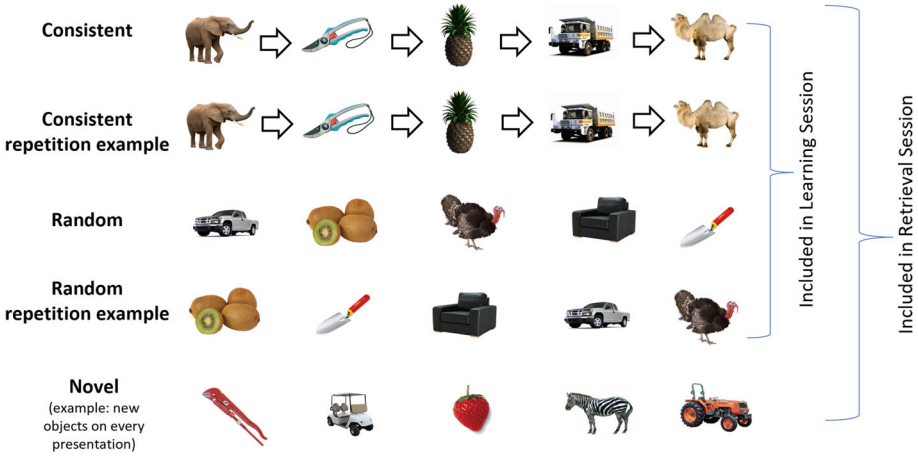

FIGURE 1 Examples of object sequences. Participants learned, and were tested on, a range of object sequences that were either consistently ordered ('consistent'; arrows indicate consistent order) or randomly ordered ('random'). Sequences of novel objects ('novel') were additionally included in the retrieval stage. Repetition examples are included to illustrate that consistent sequences had consistent object order across repetitions whereas random sequences did not.

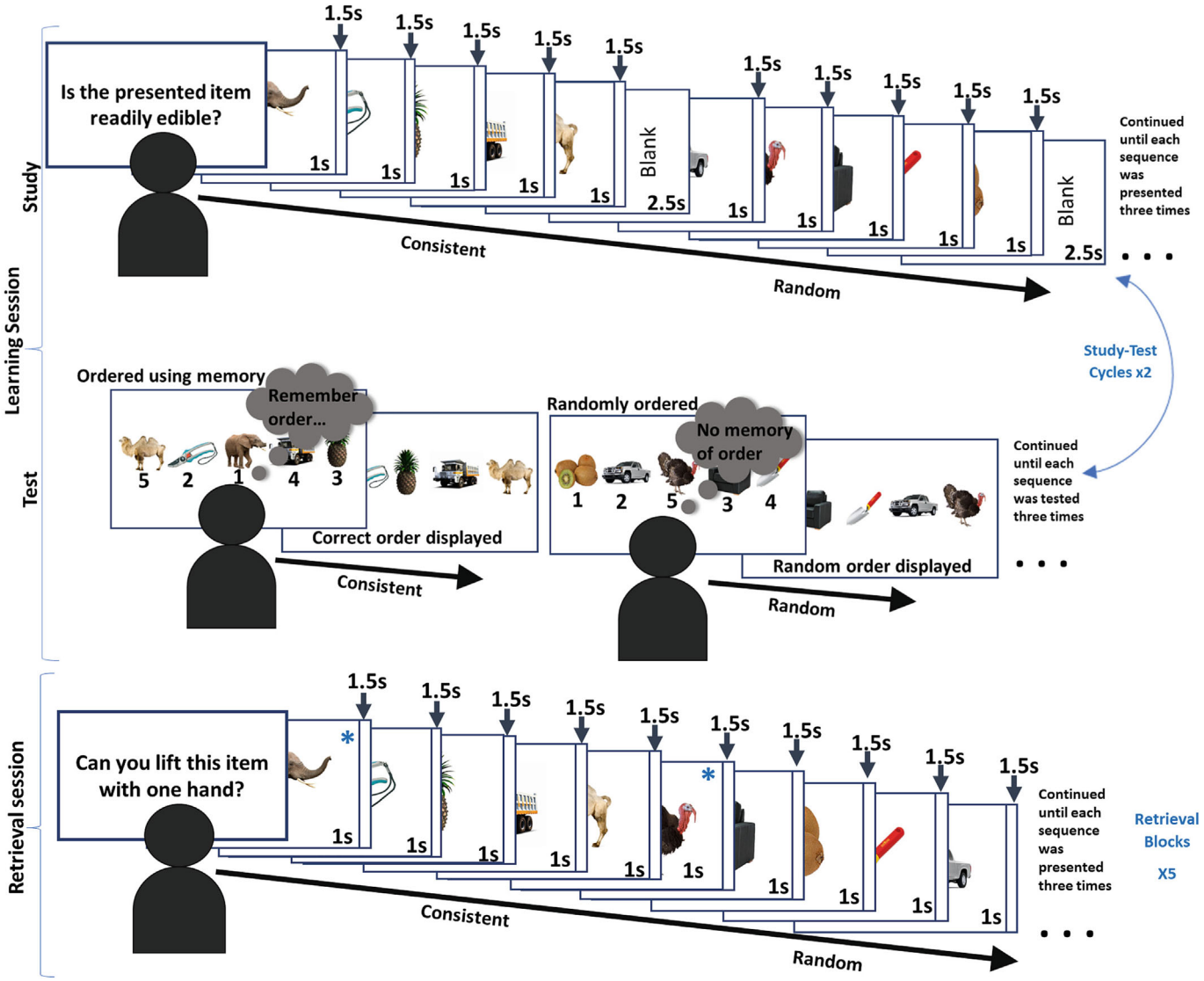

FIGURE 2 Sequence memory task layout. The task comprised a 'learning' session followed by a 'retrieval' session. Examples of the consistent and random sequences are shown. The learning session comprised study-test cycles. In the study part, participants became familiar with the object sequences by answering semantic questions about the objects presented in their sequences. In the test part, participants were asked to re-order (now randomly ordered) objects from the consistently ordered sequences. Note that the random sequences cannot be reordered correctly and participants randomly ordered the objects before being shown another random order. The sequences were shown three times within the test and study parts, and there were two study-test cycles. The retrieval session comprised five blocks, which was similar to the study part of the learning session, but all the sequences were shown seamlessly (without longer blank fixation screens). Again, participants answered semantic questions about each object displayed. Blue asterisks have been added for illustrative purposes, on some images in the retrieval session, to denote the image in position 1 of a sequence.

correct, within a sequence, was expressed as a percentage. Percentage accuracy over all the reconstruction tests was averaged to give a 'Learning Session Performance'. Note that this score was comprised of explicit measures of sequence retrieval, assessed intermittently during the learning session, with the aim of reflecting learning performance.

2.2.2 | Retrieval session

Each of the five blocks was preceded by the presentation of a yes/no semantic question (different from those used in the learning session). Each sequence was presented three times within each block (again, in a semi-randomized order to ensure that sequences of the same

type were not presented consecutively). The presentation times were the same as those in the learning session, except that the sequences were run seamlessly: Sequence boundaries were not highlighted by a longer blank fixation screen.

RTs of positions 2–5 of all trials from consistent and of all trials from random sequences were averaged, and compared, to measure the extent to which individuals utilized temporal order memory (i.e., a mnemonic representation of which items predict the next item in a sequence) to facilitate semantic judgements. This was expected to be reflected as a speeding in average response RT of the consistent sequences compared to the random sequences, 'Sequence Memory Performance' (our measure of individual differences in sequence memory) (Crivelli-Decker et al., 2018; Hsieh et al., 2014). Note that RT of position 1 of each sequence was excluded as we expected equally slow RTs for position 1 across all sequences, as items in a sequence cannot be predicted until after the first item is presented.

2.3 | MRI data acquisition

Structural and diffusion MRI data were collected using a Siemens Prisma 3T MRI system with a 32-channel head coil. Diffusion-weighted Imaging (DWI) data were acquired using a dual-shell HARDI (High Angular Resolution Diffusion-Weighted Imaging) (Tuch et al., 2002) protocol with the following parameters: slices = 80; repetition time (TR) = 9,400 ms; echo time (TE) = 67 ms; field of view (FOV) = 256 mm × 256 mm; acquisition matrix size 128 × 128; voxel dimensions = 2 × 2 × 2 mm^3; and phase encoding direction = anterior–posterior. Diffusion sensitization gradients were applied along 30 isotropic directions with a *b* value of 1,200 s/mm^2 and along 60 isotropic directions with a *b* value of 2,400 s/mm^2. Six non-diffusion-weighted images were also acquired with a *b* value of 0 s/mm^2.

T1-weighted anatomical images were obtained using a magnetization prepared rapid gradient echo scanning (MPRAGE) sequence with the following parameters: slices = 176; TR = 2,250 ms; FOV = 256 mm × 256 mm; matrix size = 256 mm × 256 mm; flip angle = 9°, TE = 3.06 ms; slice thickness = 1 mm; and voxel size: 1 × 1 × 1 mm^3.

2.4 | MRI data processing

The T1-weighted and DWI data were converted from DICOM to NIfTI formats using dcm2nii (obtained from nitrc.org). The T1-weighted data also underwent cropping, skull removal with the FSL Brain Extraction Tool (Smith, 2002) and down-sampling to a voxel size of 1.5 × 1.5 × 1.5 mm (Jenkinson et al., 2012).

Subject motion, eddy current and echo planar imaging distortions were corrected by co-registering the DWI data to their respective T1-weighted images using Explore DTI (version 4.8.3) (Leemans et al., 2009). The lower (1,200 s/mm^2) and higher (2,400 s/mm^2) *b*-value data were analysed separately. Although DTI modelling was carried out on both shells, DTI model maps from the lower *b*-value data (where the assumption of Gaussian diffusion is met; Assaf & Pasternak, 2008) were used to extract DTI scalar measures, FA (range 0–1) and Mean Diffusivity (MD, units 10^{-3} mm^2/s), radial diffusivity (RD, units 10^{-3} mm^2/s) and axial diffusivity (AD, units 10^{-3} mm^2/s) (Leemans et al., 2009; MATLAB, 2015).

To estimate the diffusion tensor in the presence of physiological noise and system-related artefacts, the Robust Estimation of Tensors by Outlier Rejection algorithm was applied (Chang et al., 2005) to the lower *b*-value data. The 'Free Water Elimination' (FWE)-DTI technique of Pasternak et al. (2009) was used to allow removal of the free water contribution to the data, improving tissue specificity. FWE is based on a dual tensor model with an isotropic tensor modelling the contribution of free water and a second tensor modelling tissue (Pasternak et al., 2009). This FWE technique was applied to the lower *b*-value data (1200) and includes spatial regularization to overcome its inherent limitations when applied to lower *b* values (less than ~2,000) (since the estimation of the model is ill-posed for single-shell acquisition) (Pasternak et al., 2009). Applying FWE is especially crucial when examining the fornix (Hoffman et al., 2022), which borders the 3rd ventricle, because contamination by CSF can erroneously influence tract DTI metrics (Kaufmann et al., 2017). Eliminating the contribution of the free-water compartment provides DTI measures that are corrected for the partial volume effect of CSF-contamination. The corrected measures improve the specificity of the DTI metrics to brain tissue (Pasternak et al., 2009). Only FWE-DTI metrics were used in the subsequent analyses. For this reason, we refer to DTI metrics with the prefix FWE- (e.g., FWE-FA) (Bauer et al., 2022).

To detect and eliminate signal artefacts in the higher *b*-value data, the Robust Estimation in Spherical Deconvolution by Outlier Rejection algorithm was applied (Parker et al., 2012). Subsequently, peaks in the fibre Orientation Density Function (fODF) in each voxel were extracted using a modified damped Richardson-Lucy deconvolution algorithm (Dell'acqua et al., 2010). Whole-brain deterministic tractography was carried out in Explore DTI (version 4.8.3) (Leemans et al., 2009). The

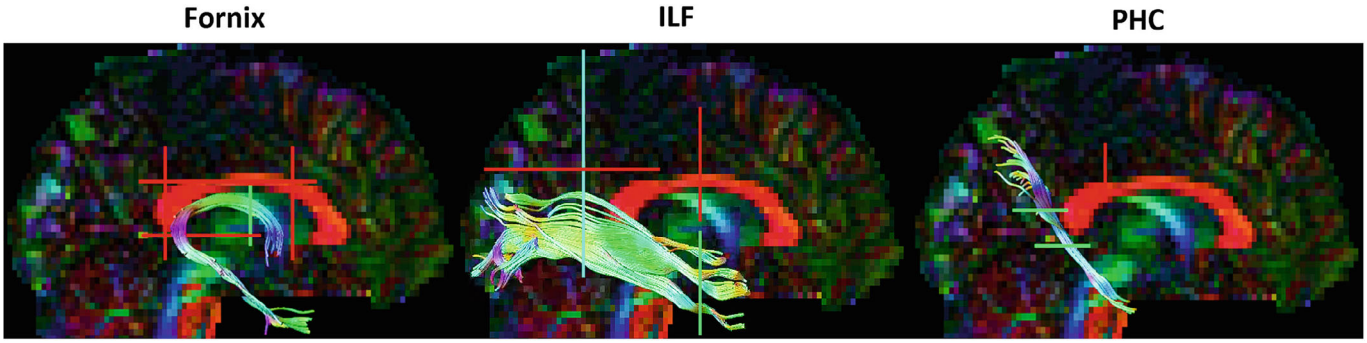

FIGURE 3 Construction of tract streamlines. Sagittal views of the fornix, ILF, and PHC streamlines constructed in an ExploreDTI example dataset (available at exploredti.com/exampledataset.htm). Right ILF and PHC tracts are shown, though they were extracted bilaterally. Colours on the brain map and the streamlines indicate diffusion along the gradient directions (left-right: red; top-bottom: blue; front-back: green). Example locations of the Boolean gates are represented by coloured lines (NOT gate: red. AND gate: green. SEED: blue). ILF, Inferior Longitudinal Fasciculus; PHC, Parahippocampal Cingulum

streamlines were constructed using an fODF amplitude threshold of .05, one seed per voxel, a step size of .5 mm and an angle threshold of 45°.

The dual-shell data were also processed to apply the biophysical NODDI model (Zhang et al., 2012), resulting in NDI (estimates the volume fraction of neurites) and ODI (estimates the variability of neurite orientation) values (both range 0–1), as well as a volume fraction of isotropic diffusion (Viso), attributed to a free water compartment. NODDI maps were created using Accelerated Microstructure Imaging via Convex Optimization (AMICO) (Daducci et al., 2015) NODDI (description and pipelines available here[2]). The resulting maps were accepted if normalized root-mean-square error map voxels in the areas of interest had error values under .3.

2.5 | Extraction of tract streamlines

To generate three-dimensional streamlines that represented the fornix, the ILF and the PHC, 'way-point' ROIs were manually drawn onto whole-brain FA maps in the diffusion space of 18 subjects, using ExploreDTI (version 4.8.3) (Figure 3). These 'way-point' ROIs allow the user to define Boolean AND and NOT gates, and SEEDS, with the aim of isolating the relevant streamlines. The protocol of Hodgetts et al. (2015) was used to extract fornix streamlines, with the exclusion of the AND gate placed on the transverse plane, as it did not appear to be required. The protocol of Wakana et al. (2007) was used to extract ILF streamlines. The protocol of Jones, Christiansen, Chapman, and Aggleton (2013) was used to extract PHC streamlines, but a NOT gate placement of Sibilia et al. (2017) was used to exclude any streamlines of the cingulum that curved forward. The resultant tracts were used to train in-house automated tractography software (Greg Parker, Cardiff University; MATLAB, 2015), which was then applied to the entire dataset. Streamlines produced by the automated tractography software were visually inspected, and spurious fibres were removed using additional NOT gates.

2.6 | Dimensionality reduction of microstructure data

FWE-FA, FWE-MD, FWE-RD, FWE-AD (from FWE-DTI), and NDI and ODI (from NODDI) values for the voxels encompassed in the tract streamlines were extracted and averaged for each tract. We did not have specific hypotheses regarding inter-hemispheric differences for the ILF or PHC, so left and right values for these tracts were averaged together. This resulted in six microstructure metrics for three tracts for all 51 participants. These diffusion measures were reduced through PCA into microstructurally informative features (Chamberland et al., 2019; Geeraert et al., 2020; see also Gagnon et al., 2022; Guberman et al., 2022; Vaher et al., 2022). The tract microstructure data were combined in a single table. The Bartlett test was used to assess the appropriateness for PCA. The *prcmp* function in R (R Core Team, 2019) was then used to apply PCA to centred and scaled data (converted to z scores). Sampling adequacy of the PCA results was tested using the Kaiser-Meyer-Olkin (KMO) test (from the R 'Psych' package; Revelle, 2022). Components were retained depending on the amount of cumulative variation they explained and on inspection of the scree plot. Following data reduction, participant scores in two biologically interpretable principal components (PCs) were used for analysis.

[2]github.com/daducci/AMICO/blob/master/doc/demos/NODDI_01.md

2.7 | Statistical analysis

For statistical testing and figure generation, R (R Core Team, 2019), RStudio (RStudio Team, 2020) and JASP (version 0.9.0.1) (JASP Team, 2021) were used. Participant datasets containing outlying values (>3 SDs from the mean) in either the behaviour condition or the microstructure PCA score data were identified and removed. *T* tests to test differences between sequence condition RTs and two-tailed Pearson's tests for correlations between performance and microstructure scores were carried out in R. To correct for multiple comparisons, *p* values were Bonferroni-corrected by dividing the standard .05 alpha level by the number of tracts: .017 (.05/3 tracts).

In addition, Bayes Factors (BFs) were calculated using the BayesFactor package in R (Morey & Rouder, 2018) and reported as BF_{10} (evidence of the alternative over the null model). To aid interpretation, BF_{10} values between 1 and 3 were taken as weak evidence in favour of the alternative model, and values exceeding 3 were taken to reflect stronger evidence (Raftery, 1995). In contrast, values between 1 and .33, and below .33, were taken as weak and stronger evidence in favour of the null, respectively (Raftery, 1995). In the cases where behavioural scores needed to be controlled for, Bayesian correlations between the residuals of variables were tested. In contrast to individual correlation tests, Bayesian multiple regression additionally allowed us to test the statistical relationships between fornix microstructure and sequence memory performance while controlling for ILF and PHC tract microstructure and learning session performance in the same model (akin to hierarchical regression). This was carried out by including the nuisance variables within the null model.

Plots were drawn using several R packages including ggcorrplot (Kassambara, 2019), ggstatsplot (Patil, 2021), ggplot2 (Wickham, 2016) and raincloudplots (Allen et al., 2019).

3 | RESULTS

3.1 | Sequence learning and memory data

3.1.1 | Learning session

Results from the reconstruction tests of the learning session showed that consistent sequences were learned reasonably well. The mean of the scores from the final repeat of the second cycle (the 6th reconstruction of a sequence) was 90.39%. To characterize participant performance during the learning session, 'Learning Session Performance' scores were created by averaging the reconstruction results across study-test cycles. The mean (and SD) of Learning Session Performance was 80.82% (16.90%).

3.1.2 | Retrieval session

The key retrieval session measure of interest, 'Sequence Memory Performance', was calculated as the difference in averaged response RTs to positions 2–5 of the sequence types random and consistent. Figure 4a shows group RT data for each position in the two sequences. Figure 4b shows that average RTs to positions 2–5 were significantly faster for items in consistent sequences than for items in random sequences ($t_{[50]} = 3.495$, $p = .001$, $d = .489$).

3.2 | Tract microstructure

Fornix, ILF and PHC streamlines were successfully recontructed in all participants. The means (and SDs) of the number of streamlines in each tract reconstruction were fornix 546.6 (119.6); ILF 615.2 (183.0); and PHC 119.1 (41.4). The means (and SDs) of the lengths in voxels of streamlines were fornix 182.7 (11.6); ILF 203.7 (9.1); and PHC 131.0 (14.9). Mean along-tract, bilaterally averaged tract microstructure metrics are shown in the Table S1. The Pearson correlation values shown in Figure 5a highlight the shared variance in these data.

The results from the PCA (overall KMO: .63, sphericity: $p < .001$; comparable to Chamberland et al., 2019; Geeraert et al., 2020) showed that 93% of the microstructure data variability was accounted for by the first two principal components, PC1 and PC2 (Figure 5; loadings shown in Table S2). PC1 accounted for 59% of the variance, and FWE-MD, FWE-RD and FWE-AD provided major negative contributions. PC1 resembled the first component found in Chamberland et al. (2019) and the second component of Geeraert et al. (2020) (see also Gagnon et al., 2022). PC1 was most influenced by MD, which, in high resolution imaging of post-mortem tissue, has been shown to strongly relate to the amount of myelin, suggesting that it is related to proportions of diffusion-restricting material (Seehaus et al., 2015). Therefore, PC1 was interpreted as positively relating to a 'tissue restriction' property of the fibres (presumably related to myelin density and axonal packing; Beaulieu, 2014). PC2 accounted for 34% of the variance, and FWE-FA and NDI provided the major negative contributions, while ODI provided a major positive

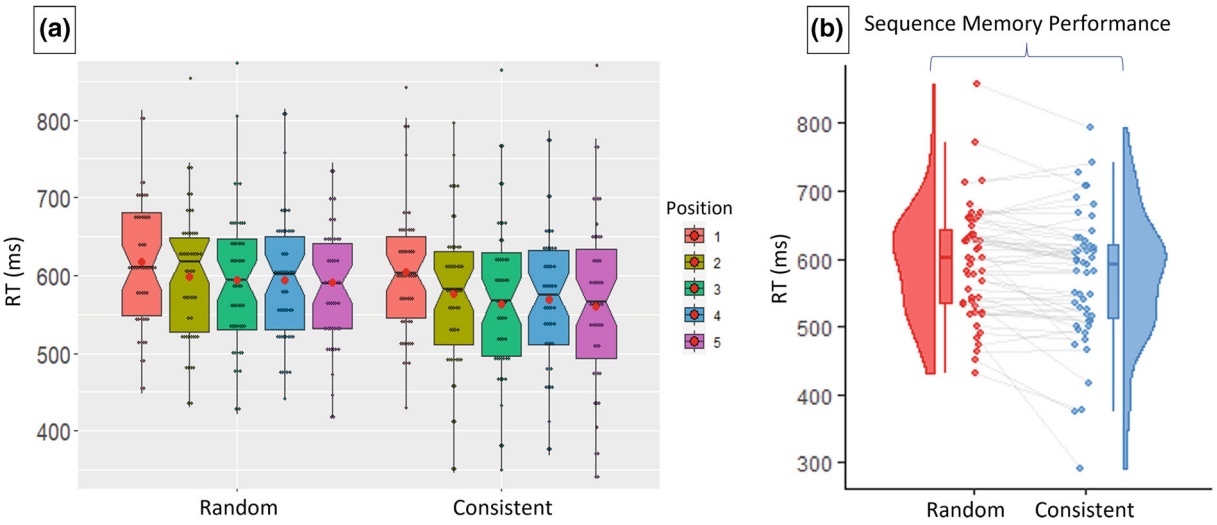

FIGURE 4 Participant averaged response RTs, for each condition. (a) Box plots of the RTs for each position in the random and consistent sequence conditions. The red dots indicate the mean values. Sequence conditions are colour coded according to the key on the right. Note that the *y*-axis range was reduced to make differences in RTs between positions clearer, so some outlying high and low individual values (grey dots) have been excluded. (b) Individual participant averaged response RTs, for positions 2–5, for the random and consistent sequence conditions. Data points from the same individuals are connected with grey lines. Sequence memory performance is the difference between random and consistent averaged RTs. Box plots and distributions are also displayed. Lines connected to the boxplots indicate 95% confidence intervals.

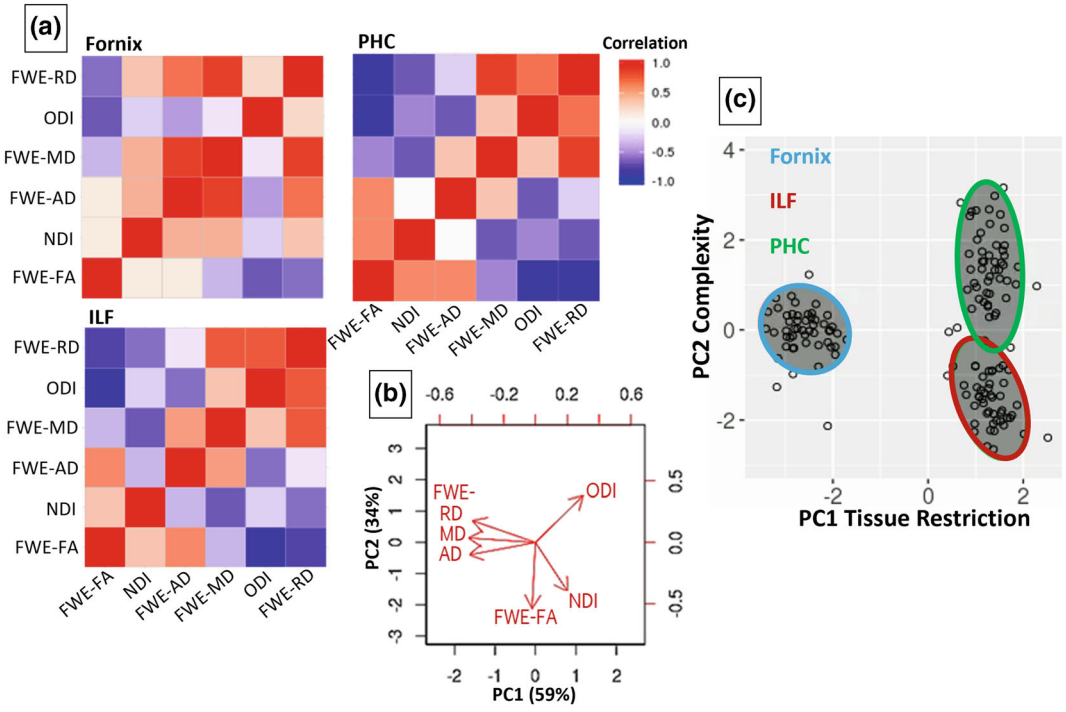

FIGURE 5 Redundancies between tract microstructure values and reduction through PCA. (a) Pearson's correlations within the microstructure data from each tract suggest that the FWE-DTI and NODDI metrics give overlapping information. Colour denotes *r* value. (b) Biplot illustrating the influence of each of the measures on PC1 and PC2, which account for 59% and 34% of the variance, respectively. (c) Tract component scores for each participant, illustrating the differing properties of the tracts. Note that one outlying PHC value lies beyond the boundaries of the graph. FWE-AD, axial diffusivity; FWE-FA, fractional anisotropy; FWE-MD, mean diffusivity; FWE-RD, radial diffusivity (with free water elimination); ILF, Inferior Longitudinal Fasciculus; PHC, Parahippocampal Cingulum; NDI, Neurite Density Index; ODI, Orientation Dispersion Index; PC, principal component

contribution. FA is not a measure of *tissue* restriction (supporting our naming of PC1, to which FA minimally contributes) but rather the degree to which mobility of water molecules is restricted to any single direction (diffusion restriction). It is often found to correlate more strongly with ODI (negatively) than NDI (e.g., Churchill et al., 2017; Pines et al., 2020; Zhang et al., 2012), suggesting that dispersion of fibres influences the anisotropy measurement in a voxel more than the tissue properties themselves. Indeed, FA has been shown to relate most strongly to fibre orientations in high resolution imaging of post-mortem tissue (Seehaus et al., 2015). Therefore, since ODI is lower in tracts known to have greater fibre coherency and higher in tracts known to have more fibre fanning and crossing (Mollink et al., 2017; Zhang et al., 2012), and FA can be influenced by how coherently fibres within a voxel are organized (Jones, Knosche, & Turner, 2013; Pierpaoli et al., 1996), PC2 was interpreted as relating to a 'complexity' property of the fibres (the dispersion of modelled fibre orientations) (Schilling et al., 2018). Note that PC2 scores were sign-flipped, so that larger PC2 scores indicated greater complexity, to facilitate interpretation.

3.3 | Relationships between sequence memory and tract microstructure

As is often the case with real/social science data (Bono et al., 2017), Sequence Memory Performance was non-normally distributed (right skew, >1) so, to allow the use of parametric testing throughout the analyses, the data were transformed. A constant (of the most negative value, sign-flipped and rounded up) was added to each value, and the square root was then calculated (McDonald, 2014), resulting in normally shaped data. Unless stated otherwise, 'Sequence Memory Performance' henceforth refers to the transformed data.

As the Extended Hippocampal System is known to be important for episodic memory (Aggleton & Brown, 1999; Gaffan & Hornak, 1997), we hypothesized that individual differences in fornix microstructure, which may reflect a quality of information flow between regions of this system (Jankowski et al., 2013), would relate to individual differences in sequence memory.

In line with our hypothesis, there was a significant positive correlation between Sequence Memory Performance and fornix PC2 (indexing microstructural complexity) (such that better item-in-sequence memory, indexed by a greater difference in RT between random and consistently ordered, learned sequences, was associated with higher complexity scores), and the resulting BF indicated evidence in favour of the alternative model ($r_{[46]} = .343$, $p = .017$, $BF_{10} = 4.16$). The correlation with fornix PC1 (indexing tissue restriction), however, was not significant ($r_{[46]} = .029$, $p = .847$, $BF_{10} = .33$).

There were no significant correlations between Sequence Memory Performance and ILF PC1/PC2 ($r_{(46)} = .030$, $p = .839$, $BF_{10} = .33$; $r_{(46)} = .053$, $p = .720$, $BF_{10} = .34$) or PHC PC1/PC2 ($r_{(46)} = -.014$, $p = .923$, $BF_{10} = .33$; $r_{(46)} = .116$, $p = .433$, $BF_{10} = .43$). These results indicate that microstructure of the fornix, specifically the 'complexity' component (PC2), relates to memory of objects in temporal context whereas microstructure properties of the ILF and PHC do not.

Moreover, the correlation between Sequence Memory Performance and fornix complexity held when controlling for Learning Session Performance ($r_{[44]} = .369$, $p = .011$, $BF_{10} = 6.11$), indicating that this fornix property may be specifically important for sequence retrieval. There was also no significant correlation between Sequence Memory Performance and Learning Session Performance ($r_{[45]} = .259$, $p = .079$, $BF_{10} = 1.31$). Moreover, there continued to be no significant correlations between Sequence Memory Performance and fornix tissue restriction, ILF tissue restriction/complexity or PHC tissue restriction/complexity, when controlling for Learning Session Performance (Figure 6a).

Bayesian multiple regression analysis, comparing models with fornix PC2, PHC PC2, ILF PC2 as predictors of Sequence Memory Performance, with Learning Session Performance included in the null model, indicated that a model with only fornix PC2 (complexity) was most probable ($BF_{10} = 5.297$, against the null model). Model averaging indicated that the data were most likely under a model that included fornix PC2 ($BF_{inclusion} = 4.833$). The inclusion probabilities figure (Figure 6b) shows that only fornix PC2 has a greater marginal inclusion probability than the prior inclusion probability, indicating its importance for prediction. In a separate test where PHC PC2, ILF PC2 and Learning Session Performance were all included in the null model, evidence for the importance of fornix PC2 held ($BF_{10}/BF_{inclusion} = 4.051$).

These findings indicate the relative importance of the fornix, compared with the PHC and ILF, especially the fibre complexity component (PC2) of this tract, for memory of objects in temporal context.

For completeness, results of correlation tests between the behavioural scores and raw tract microstructure values are shown in Figure S1.

4 | DISCUSSION

The hippocampus has been shown to play a crucial role in the construction and retrieval of representations of

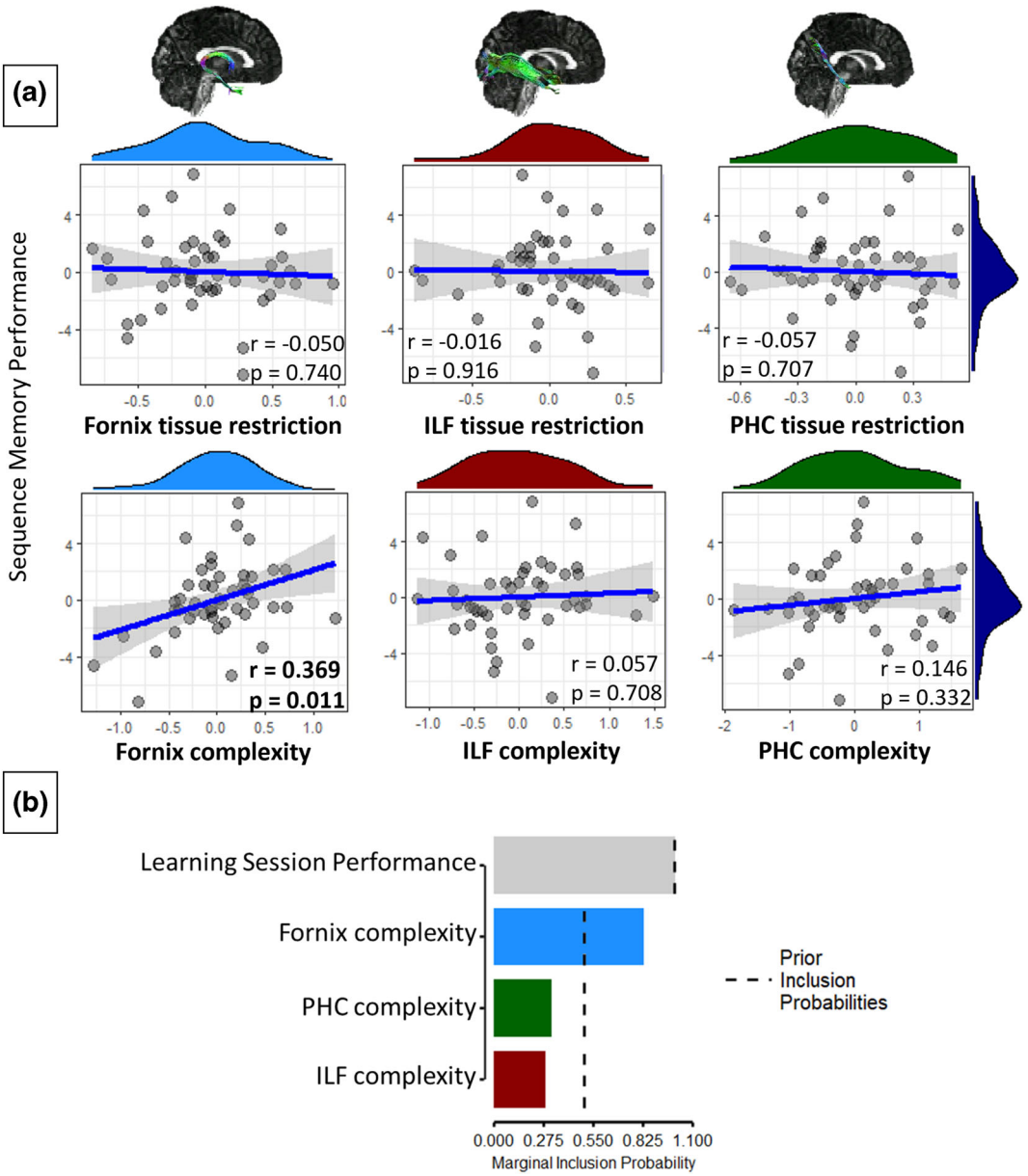

FIGURE 6 Associations between tract microstructure scores and sequence memory performance. (a) Correlation plots between sequence memory performance and microstructure scores, when controlling for learning session performance. The light-blue histograms show the distributions of the fornix tissue restriction/complexity data. The green and red histograms show the distributions of the PHC tissue restriction/complexity data and ILF tissue restriction/complexity data, respectively. The dark blue histograms show the distribution of sequence memory performance. The blue lines are the regression lines, and surrounding shaded areas represent the 95% confidence interval. There was a significant partial correlation between sequence memory performance and fornix complexity (at alpha threshold .017). Example fornix, ILF and PHC streamlines are shown on template brains. (b) Bar graph of the posterior inclusion probabilities of the Bayesian linear regression, predicting sequence memory performance with variables fornix complexity, ILF complexity, PHC complexity and learning session performance. The dashed line indicates the prior inclusion probabilities. ILF, Inferior Longitudinal Fasciculus; PHC, Parahippocampal Cingulum

events associated through their temporal contiguity (Davachi & DuBrow, 2015; Howard & Eichenbaum, 2015; Ranganath & Hsieh, 2016; Schapiro et al., 2016). Complementing this finding, here, we demonstrate that microstructure of the fornix—a white matter tract that interconnects an extended hippocampal system, including the hippocampus, anterior thalamic nucleus, mamillary bodies, septal nuclei and medial prefrontal cortex—predicts individual differences in temporal sequence memory in humans. These results lend credence to the idea that hippocampal contributions to memory may be supported by an extended network that

is linked via the fornix (Aggleton, 2012; Aggleton & Brown, 1999; Bubb et al., 2017; Gaffan, 1992; Gaffan & Hornak, 1997).

Previously, through representational similarity analysis of fMRI signals recorded during the retrieval phase of a sequence memory task, Hsieh et al. (2014) demonstrated that individual differences in hippocampal voxel pattern information correlated with RT indices of sequence learning. Using scalp electroencephalography (EEG) recordings with the same task, Crivelli-Decker et al. (2018) showed that changes in oscillatory activity in the theta band (4–7 Hz) predicted sequence learning in this paradigm. Our findings complement these prior results in revealing that microstructure properties of the fornix, in particular a property putatively reflecting fibre complexity (Chamberland et al., 2019), correlated with inter-individual RT difference between consistent and random sequences, indexing the extent to which, after a sequence has been learned, individuals use that sequence memory to facilitate response preparation by predicting upcoming objects during consistent sequences, thus resulting in faster semantic decisions (Davachi & DuBrow, 2015; Williams et al., 2023). These findings confirm the importance of the hippocampus's structural connectivity in supporting successful sequence memory.

Notably, in the Hsieh et al. (2014) paradigm, activity patterns in the parahippocampal cortex and perirhinal cortex (bilaterally) carried information about temporal position and object identity respectively, but the hippocampus uniquely carried conjunctive representations of item and temporal position (see also Gaffan & Parker, 1996, Parker & Gaffan, 1997 for comparable evidence of a unique role for the primate fornix in integrating information about objects and their positions in space). Our results align with this by supporting a unique role of the fornix in item-in-temporal sequence memory. We found no evidence to suggest that microstructure properties of the ILF or PHC related to sequence memory, and the Bayes factors of these correlations indicated (albeit weak) evidence in favour of the null. Moreover, supporting the unique role of the fornix, Bayesian multiple regression analysis, comparing models with fornix, PHC and ILF complexity scores as predictors of Sequence Memory Performance (with Learning Session Performance included in the null model) indicated that a model with only fornix complexity was most probable, and model averaging indicated that the data were most likely under models including fornix complexity. This preponderance of evidence supports the idea that memory for items in temporal context is supported specifically by an extended hippocampal system.

The fornix contains bidirectional pathways supporting direct hippocampal connections within the extended hippocampal system (Aggleton et al., 2010; Aggleton et al., 2015; Aggleton & Brown, 1999; Bubb et al., 2017). The fornix may contribute to hippocampal functioning by conveying theta rhythms, the prominent oscillation band of the hippocampus (Buzsaki, 2002), through this system (Aggleton et al., 2010; Jankowski et al., 2013). The fornix directly connects the hippocampus to: the septum/diagonal band of Broca, which supports the generation of theta activity (Leao et al., 2015; Swanson & Cowan, 1979); the supramammillary area, which has been shown to influence the frequency of hippocampal theta (Kirk, 1998; Pan & McNaughton, 2004), and the anterior thalamic nuclei, which not only operate in conjunction with the hippocampus through theta interactions but also modulate hippocampal theta (Żakowski et al., 2017). The fornix also connects the hippocampus to the medial prefrontal cortex (Aggleton et al., 2015), a region also implicated in the sequential binding of items within events (Davachi & DuBrow, 2015). The fornix may be both delivering theta rhythms to the hippocampus and facilitating hippocampal influence on extended hippocampal system theta. For example, fornix transection, disconnecting the septum from the hippocampus, abolishes hippocampal theta (Rawlins et al., 1979), while stimulating the fornical input from the hippocampus to anterior thalamic nuclei modulates thalamic theta (Jankowski et al., 2013; Tsanov et al., 2011).

Hippocampal theta is understood to be critical to the temporal organization of active neuronal ensembles (Buzsaki, 2002) and may therefore support temporal organization of episodic memory (Buzsáki & Moser, 2013; Eichenbaum, 2017: Herweg et al., 2020; Lisman & Redish, 2009; Skaggs et al., 1996). One specific proposal is that theta oscillations, which provide time windows for fast-acting long-term potentiation (LTP) and depression (LTD), mediate item-context binding (see Hanslmayr & Staudigl, 2014 for discussion). Indeed, MTL theta phase coding is evident in humans learning image sequences (Reddy et al., 2021). Moreover, using electroencephalography in conjunction with a sequence memory task like that used by Hsieh et al., and in the current study, Crivelli-Decker et al. (2018) showed frontal midline theta power (which may be influenced by hippocampal theta, Hsieh & Ranganath, 2014, through connections mediated by the fornix, Aggleton et al., 2015), to be lower during items in consistent sequences than during items in random sequences. Additionally, decreases in frontal midline theta power (which may reflect elevated theta connectivity, Solomon et al., 2019) correlated with RT of semantic decisions on upcoming objects in consistent sequences (Crivelli-Decker et al., 2018). It may be that hippocampus-influenced frontal midline theta aids coding of temporal information specifically, rather than

temporal and spatial information, as temporal duration and not spatial distance has been shown to relate to frontal midline theta power modulation (Liang et al., 2021). Together, these results clearly link theta activity with encoding and retrieval of sequence memory. Therefore, sequence memory may rely on inter-regional functional communication within and beyond the extended hippocampal system, mediated by theta connectivity conveyed by the fornix, the latter in line with the findings from our study.

However, our interpretation, that is, the fornix supports sequence memory through its role in communication of theta-based processes between the hippocampus and an extended hippocampal system, is likely incomplete. One shortcoming is that the precise relationship between inter-regional theta synchronization and local activity is not currently well understood (Solomon et al., 2019). Furthermore, the fornix also carries some (albeit light) non-hippocampal connections, including those between the entorhinal cortex and the anterior thalamic nuclei (Saunders & Aggleton, 2007; Saunders et al., 2005), both of which have been shown to conduct forms of temporal coding (Bellmund et al., 2019; Nelson, 2021). Future studies could incorporate measurement of extended hippocampal theta rhythms into this study design and test for relationships between individual differences in hippocampal theta modulation, the extent of theta-based communication (e.g., phase/amplitude coupling), fornix microstructure and sequence retrieval performance. However, this may require invasive recording (e.g., Solomon et al., 2018), as measuring electrophysiological signals from deep sources non-invasively with magnetoencephalography, for example, is possible but it would be challenging to distinguish the individual regions of this extended hippocampal network (Pu et al., 2018).

In this study, extending previous work from our lab that focused on DTI measures, we adopted a recently developed dimensionality reduction framework to take advantage of redundancies in dMRI measures (Chamberland et al., 2019; Geeraert et al., 2020; see also Guberman et al., 2022; Gagnon et al., 2022). By combining multiple measures through PCA (Chamberland et al., 2019; Geeraert et al., 2020), we found that the two major components, PC1 and PC2, were contributed to mostly by FWE-MD, FWE-RD and FWE-AD and FWE-FA, NDI and ODI, respectively. We therefore considered these components to capture the properties of tissue restriction and complexity, respectively. The PCA components reported in this study share similarities with those reported in previous studies (Chamberland et al., 2019; Geeraert et al., 2020). PC1 is similar to the first component reported in Chamberland et al. (2019), which was also named 'restriction' and was negatively influenced by RD and positively influenced by a measure of fibre density. PC1 is also similar to the second component in Geeraert et al. (2020), named 'myelin and axonal packing' and influenced negatively by RD and MD and positively by NDI. PC2 overlaps with the first component in Geeraert et al. (2020), which they named 'tissue complexity' because it was influenced positively by FA and negatively by ODI. Although there are minor differences in the resulting components across studies (as would be expected when there are differences in the microstructure measures and tracts considered), the commonalities in the components confirm the usefulness of microstructure data reduction as a method to characterize tract properties.

The positive correlation between fornix PC2 and our RT difference index of sequence memory suggests that increased fornix tissue complexity (reduced fornix axon coherence) relates to better sequence memory (as indexed by faster RTs when making semantic decisions about objects in consistent vs. random sequences). The causes of inter-individual variation in white matter microstructure are not fully understood but presumably reflect both environmental and genetic influences (Cahn et al., 2021; Luo et al., 2022). Studies examining white matter FA and ODI over age indicate that tissue complexity changes during early development, perhaps supporting development of complex behaviours. For example, scores on the tissue complexity component in Geeraert et al. (2020) increased with age in children. Positive and negative correlations have also been identified in children between white-matter ODI and reading skill and between FA and reading skill, respectively (Huber et al., 2019), suggesting increased tissue complexity is linked to better performance, even when controlling for age. Since our cohort comprises young adults, an age group in which age-related FA increases plateau and age-related ODI increases are slower than that of older adults (Chang et al., 2015), it is likely that we captured stable, peak inter-individual differences in fornix complexity. Related findings have linked increased white matter fibre complexity (i.e., lower FA values) to better scene/place memory (Gomez et al., 2015; Tavor et al., 2014) (see also Giacosa et al., 2016, for links between reduced fibre coherence and acquired expertise in adults). Further, improvement on a car-racing game in humans (and on the Morris water maze in 4 months old rats) led to FA decreases in the fornix (Hofstetter et al., 2013). One possibility is that fornix complexity reflects individual differences in the extent to which fornix axons disperse to reach target sites (Mathiasen et al., 2019; Poletti & Creswell, 1977). There is evidence that variation in microstructural properties of white matter tracts can

influence the timing of neural signalling that maintains oscillatory neural activity within and between neural "coalitions" (Bells et al., 2019). Individual differences in fornix microstructure may therefore influence the precise frequency (or other properties) of theta rhythmicity and hence individual differences in the efficiency of theta-mediated item-context binding (McNaughton et al., 2006).

A limitation with this study is that the sample used was entirely female, reflecting the availability of a participant sample for this work. We have no predictions about sex differences in temporal memory, so we anticipate that inclusion of male participants would result in similar findings, and consistent with this, previous work examining fornix microstructure and memory performance in young healthy adults reported no effects of participant sex (Hodgetts et al., 2020; see also Cahn et al., 2021). Considering our tractography methods, it should be noted that although the individual diffusion metrics used here have been histologically validated independently (Sato et al., 2017; Schilling et al., 2018), components resulting from their reduction with PCA have not (Gagnon et al., 2022; Geeraert et al., 2020). It is not clear, therefore, that any one underlying tract property would be wholly reflected in one component (i.e., complexity could influence PC2, but it could also influence PC1 to a lesser extent). Furthermore, virtual tract renditions are created from estimations of water diffusion directionality, not from the anatomy itself, and characterization of fibres is limited by the MRI technique (e.g., the magnetic gradient amplitudes determine resolution thereby limiting the minimum detectable fibre diameter; McNab et al., 2013). Although we constructed virtual tract renditions using anatomical knowledge and were informed by previous research, it is not possible to test the specificity of the tractography methods, for each participant, without knowing the true underlying anatomy (Schilling et al., 2020).

Relatedly, it is possible that our approach to structure–function relationships is too anatomically coarse. We chose to construct the ILF as a single bundle in line with established and reproducible protocols (see also Bullock et al., 2022; Radwan et al., 2022). However, the ILF may be divided into distinct sub-bundles, only some of which are relevant to object-in-sequence memory. While there is no established protocol for structurally subdividing the ILF (Herbet et al., 2018; Latini et al., 2017; Panesar et al., 2018), a different approach, which combines fMRI and dMRI to identify functionally defined white matter sub-bundles (fSuB) (Grotheer et al., 2022), may prove useful in future studies. That said, previous work from our group has shown the clear functional relevance of the ILF treated as a unified bundle to object and semantic cognition (Hodgetts et al., 2015, 2017), suggesting our (weak) null findings for the ILF may not simply be due to a lack of functional relevance of the ILF considered in its entirety.

Similarly, we averaged across right and left ILF and PHC tract values. While this may also have contributed to the null findings for the ILF and PHC, in particular as the ILF has been shown to have lateralized properties (e.g., Latini et al., 2017), we did not have specific hypotheses regarding finding inter-hemispheric differences for the ILF or PHC because the previous fMRI study of this paradigm did not find significant differences between left and right PrC and parahippocampal cortex for coding of object and sequence information respectively (Hsieh et al., 2014). Increasing the number of tract-behaviour correlation tests, by testing left and right ILF and PHC tract values separately, would have increased the chance of type 1 error, or type 2 errors if we corrected for the increased number of tests. Moreover, our previous work on the link between ILF microstructure and object and semantic cognition included bilateral ILF metrics and found relationships between microstructure and cognition (Hodgetts et al., 2015, 2017), one of which found no significant inter-hemispheric differences (Hodgetts et al., 2017) and the other found behaviour-microstructure correlations bilaterally (Hodgetts et al., 2015).

Lastly, it should be noted that although we have shown a relationship between fornix microstructure and performance during the retrieval phase (Sequence Memory Performance) independent of performance during the initial learning phase (Learning Phase performance), we do not conclude that fornix microstructure selectively influences retrieval and not learning of sequences, rather that it may influence learning *and* retrieval of sequences (see, e.g., Postans et al., 2014; Hodgetts et al., 2020, for evidence of a role of fornix microstructure in spatial learning). Unfortunately, due to the task design, we do not have a more sensitive measure of learning. For example, we could not perform slope analyses on RT improvements over sequence repetitions in the learning phase (see Hodgetts et al., 2020) because the semantic question changed at the third repetition, thereby causing an increase in RT halfway through the repetitions.

In summary, this study demonstrated the specific importance of the fornix in supporting memory of objects within a temporal context, extending previous work demonstrating the importance of the hippocampus as a key region supporting binding of spatial–temporal information (Davachi & DuBrow, 2015; Graham et al., 2010; Ranganath, 2010). Furthermore, and going beyond previous DTI studies, use of a recently developed microstructure dimensionality reduction technique allowed us to

posit that fornix fibre complexity may underlie inter-individual variation in sequence memory performance, potentially by mediating individual differences in theta-mediated network communication efficiency/complexity within an extended hippocampal-fornix system critical for episodic memory.

AUTHOR CONTRIBUTIONS

Marie-Lucie Read: Data curation; formal analysis; writing - original draft; writing - review and editing. **Katja Umla-Runge:** Conceptualization; investigation; project administration; resources; supervision; writing - original draft; writing - review and editing. **Andrew Lawrence:** Resources; supervision; writing - original draft; writing - review and editing. **Alison G. Costigan:** Investigation; writing - original draft; writing - review and editing. **Liang-Tien Hsieh:** Methodology; writing - original draft. **Maxime Chamberland:** Methodology; writing - original draft; writing - review and editing. **Charan Ranganath:** Conceptualization; supervision; writing - original draft; writing - review and editing. **Kim S. Graham:** Conceptualization; resources; supervision; writing - original draft; writing - review and editing.

ACKNOWLEDGEMENTS

We would like to thank Matt Jones and Angharad Williams for their help with initial data curation, Ashvanti Valji for her help with data collection, Greg Parker for the use of his Automated Tractography Software and Ofer Pasternak and Greg Parker for the implementation of the free-water correction pipeline.

CONFLICT OF INTEREST STATEMENT

There is no conflict of interest associated with this publication.

DATA AVAILABILITY STATEMENT

The raw neuroimaging data cannot be shared publicly due to ethical restrictions relating to General Data Protection Regulation. These do not allow for the public archiving of study data. Access to pseudo-anonymized data may be granted, however, after the signing and approval of suitable data-transfer agreements. Readers seeking access through this mechanism should contact Professor Andrew Lawrence, the data controller, at the Cardiff University Brain Research Imaging Centre (lawrencead@cardiff.ac.uk).

PEER REVIEW

The peer review history for this article is available at https://publons.com/publon/10.1111/ejn.15940.

ORCID

Marie-Lucie Read https://orcid.org/0000-0003-4809-5937
Katja Umla-Runge https://orcid.org/0000-0002-9615-8907
Andrew D. Lawrence https://orcid.org/0000-0001-6705-2110
Alison G. Costigan https://orcid.org/0000-0002-9164-3081
Maxime Chamberland https://orcid.org/0000-0001-7064-0984
Kim S. Graham https://orcid.org/0000-0002-1512-7667

REFERENCES

Aggleton, J. P. (2012). Multiple anatomical systems embedded within the primate medial temporal lobe: Implications for hippocampal function. *Neuroscience and Biobehavioral Reviews*, *36*(7), 1579–1596. https://doi.org/10.1016/j.neubiorev.2011.09.005

Aggleton, J. P., & Brown, M. W. (1999). Episodic memory, amnesia, and the hippocampal-anterior thalamic axis. *The Behavioral and Brain Sciences*, *22*(3), 425–444; discussion 444–489. https://doi.org/10.1017/S0140525X99002034

Aggleton, J. P., & Brown, M. W. (2005). Contrasting hippocampal and perirhinal cortex function using immediate early gene imaging. *The Quarterly Journal of Experimental Psychology. B*, *58*(3–4), 218–233. https://doi.org/10.1080/02724990444000131

Aggleton, J. P., O'Mara, S. M., Vann, S. D., Wright, N. F., Tsanov, M., & Erichsen, J. T. (2010). Hippocampal–anterior thalamic pathways for memory: Uncovering a network of direct and indirect actions. *The European Journal of Neuroscience*, *31*(12), 2292–2307. https://doi.org/10.1111/j.1460-9568.2010.07251.x

Aggleton, J. P., Wright, N. F., Rosene, D. L., & Saunders, R. C. (2015). Complementary patterns of direct amygdala and hippocampal projections to the macaque prefrontal cortex. *Cerebral Cortex*, *25*(11), 4351–4373. https://doi.org/10.1093/cercor/bhv019

Allen, M., Poggiali, D., Whitaker, K., Marshall, T. R., & Kievit, R. A. (2019). Raincloud plots: A multi-platform tool for robust data visualization. *Wellcome Open Research*, *4*, 63. https://doi.org/10.12688/wellcomeopenres.15191.1

Assaf, Y., Johansen-Berg, H., & Thiebaut de Schotten, M. (2019). The role of diffusion MRI in neuroscience. *NMR in Biomedicine*, *32*(4), e3762. https://doi.org/10.1002/nbm.3762

Assaf, Y., & Pasternak, O. (2008). Diffusion tensor imaging (DTI)-based white matter mapping in brain research: A review. *Journal of Molecular Neuroscience*, *34*(1), 51–61. https://doi.org/10.1007/s12031-007-0029-0

Bauer, C. E., Zachariou, V., Maillard, P., Caprihan, A., & Gold, B. T. (2022). Multi-compartment diffusion magnetic resonance imaging models link tract-related characteristics with working memory performance in healthy older adults. *Frontiers in Aging Neuroscience*, *14*, 995425. https://doi.org/10.3389/fnagi.2022.995425

Beaulieu, C. (2002). The basis of anisotropic water diffusion in the nervous system—A technical review. *NMR in Biomedicine*, *15*(7–8), 435–455. https://doi.org/10.1002/nbm.782

Beaulieu, C. (2014). Chapter 8—The biological basis of diffusion anisotropy. In H. Johansen-Berg & T. E. J. Behrens (Eds.), *Diffusion MRI (second edition)* (Second ed., pp. 155–183). Academic Press. https://doi.org/10.1016/B978-0-12-396460-1.00008-1

Bellmund, J. L., Deuker, L., & Doeller, C. F. (2019). Mapping sequence structure in the human lateral entorhinal cortex. *eLife*, *8*, e45333. https://doi.org/10.7554/eLife.45333

Bells, S., Cercignani, M., Deoni, S., Assaf, Y., Pasternak, O., Evans, C. J., Leemans, A., & Jones, D. K. (2011). Tractometry–comprehensive multi-modal quantitative assessment of white matter along specific tracts. In Proc. ISMRM (Vol. 678, p. 1).

Bells, S., Lefebvre, J., Longoni, G., Narayanan, S., Arnold, D. L., Yeh, E. A., & Mabbott, D. J. (2019). White matter plasticity and maturation in human cognition. *Glia*, *67*(11), 2020–2037. https://doi.org/10.1002/glia.23661

Benear, S. L., Ngo, C. T., & Olson, I. R. (2020). Dissecting the fornix in basic memory processes and neuropsychiatric disease: A review. *Brain Connectivity*, *10*(7), 331–354. https://doi.org/10.1089/brain.2020.0749

Bono, R., Blanca, M. J., Arnau, J., & Gómez-Benito, J. (2017). Non-normal distributions commonly used in health, education, and social sciences: A systematic review. *Frontiers in Psychology*, *8*, 1602. https://doi.org/10.3389/fpsyg.2017.01602

Bourbon-Teles, J., Jorge, L., Canário, N., & Castelo-Branco, M. (2021). Structural impairments in hippocampal and occipito-temporal networks specifically contribute to decline in place and face category processing but not to other visual object categories in healthy aging. *Brain and Behavior: A Cognitive Neuroscience Perspective*, *11*(8), e02127. https://doi.org/10.1002/brb3.2127

Bubb, E. J., Kinnavane, L., & Aggleton, J. P. (2017). Hippocampal - diencephalic - cingulate networks for memory and emotion: An anatomical guide. *Brain and Neuroscience Advances*, *1*(1), 239821281772344. https://doi.org/10.1177/2398212817723443

Bubb, E. J., Metzler-Baddeley, C., & Aggleton, J. P. (2018). The cingulum bundle: Anatomy, function, and dysfunction. *Neuroscience and Biobehavioral Reviews*, *92*, 104–127. https://doi.org/10.1016/j.neubiorev.2018.05.008

Bullock, D. N., Hayday, E. A., Grier, M. D., Tang, W., Pestilli, F., & Heilbronner, S. R. (2022). A taxonomy of the brain's white matter: Twenty-one major tracts for the 21st century. *Cerebral Cortex*, *32*(20), 4524–4548. https://doi.org/10.1093/cercor/bhab500

Buzsaki, G. (2002). Theta oscillations in the hippocampus. *Neuron*, *33*(3), 325–340. https://doi.org/10.1016/S0896-6273(02)00586-X

Buzsáki, G., & Moser, E. I. (2013). Memory, navigation and theta rhythm in the hippocampal-entorhinal system. *Nature Neuroscience*, *16*(2), 130–138. https://doi.org/10.1038/nn.3304

Cahn, A. J., Little, G., Beaulieu, C., & Tétreault, P. (2021). Diffusion properties of the fornix assessed by deterministic tractography shows age, sex, volume, cognitive, hemispheric, and twin relationships in young adults from the human connectome project. *Brain Structure & Function*, *226*(2), 381–395. https://doi.org/10.1007/s00429-020-02181-9

Catani, M., Jones, D. K., Donato, R., & Ffytche, D. H. (2003). Occipito-temporal connections in the human brain. *Brain*, *126*(Pt 9), 2093–2107. https://doi.org/10.1093/brain/awg203

Chamberland, M., Raven, E. P., Genc, S., Duffy, K., Descoteaux, M., Parker, G. D., Tax, C. M. W., & Jones, D. K. (2019). Dimensionality reduction of diffusion MRI measures for improved tractometry of the human brain. *NeuroImage*, *200*, 89–100. https://doi.org/10.1016/j.neuroimage.2019.06.020

Chang, L. C., Jones, D. K., & Pierpaoli, C. (2005). RESTORE: Robust estimation of tensors by outlier rejection. *Magnetic Resonance in Medicine*, *53*(5), 1088–1095. https://doi.org/10.1002/mrm.20426

Chang, Y. S., Owen, J. P., Pojman, N. J., Thieu, T., Bukshpun, P., Wakahiro, M. L., Berman, J. I., Roberts, T. P. L., Nagarajan, S. S., Sherr, E. H., & Mukherjee, P. (2015). White matter changes of neurite density and fiber orientation dispersion during human brain maturation. *PLoS ONE*, *10*(6), e0123656. https://doi.org/10.1371/journal.pone.0123656

Charles, D. P., Gaffan, D., & Buckley, M. J. (2004). Impaired recency judgments and intact novelty judgments after fornix transection in monkeys. *The Journal of Neuroscience*, *24*(8), 2037–2044. https://doi.org/10.1523/jneurosci.3796-03.2004

Churchill, N. W., Caverzasi, E., Graham, S. J., Hutchison, M. G., & Schweizer, T. A. (2017). White matter microstructure in athletes with a history of concussion: Comparing diffusion tensor imaging (DTI) and neurite orientation dispersion and density imaging (NODDI). *Human Brain Mapping*, *38*(8), 4201–4211. https://doi.org/10.1002/hbm.23658

Coad, B. M., Postans, M., Hodgetts, C. J., Muhlert, N., Graham, K. S., & Lawrence, A. D. (2020). Structural connections support emotional connections: Uncinate fasciculus microstructure is related to the ability to decode facial emotion expressions. *Neuropsychologia*, *145*, 106562. https://doi.org/10.1016/j.neuropsychologia.2017.11.006

Crivelli-Decker, J., Hsieh, L. T., Clarke, A., & Ranganath, C. (2018). Theta oscillations promote temporal sequence learning. *Neurobiology of Learning and Memory*, *153*(Pt A), 92–103. https://doi.org/10.1016/j.nlm.2018.05.001

Daducci, A., Canales-Rodriguez, E. J., Zhang, H., Dyrby, T. B., Alexander, D. C., & Thiran, J. P. (2015). Accelerated microstructure imaging via convex optimization (AMICO) from diffusion MRI data. *NeuroImage*, *105*, 32–44. https://doi.org/10.1016/j.neuroimage.2014.10.026

Davachi, L., & DuBrow, S. (2015). How the hippocampus preserves order: The role of prediction and context. *Trends in Cognitive Sciences*, *19*(2), 92–99. https://doi.org/10.1016/j.tics.2014.12.004

de Santis, S., Drakesmith, M., Bells, S., Assaf, Y., & Jones, D. K. (2014). Why diffusion tensor MRI does well only some of the time: Variance and covariance of white matter tissue microstructure attributes in the living human brain. *NeuroImage*, *89*, 35–44. https://doi.org/10.1016/j.neuroimage.2013.12.003

Dell'acqua, F., Scifo, P., Rizzo, G., Catani, M., Simmons, A., Scotti, G., & Fazio, F. (2010). A modified damped Richardson-Lucy algorithm to reduce isotropic background effects in spherical deconvolution. *NeuroImage*, *49*(2), 1446–1458. https://doi.org/10.1016/j.neuroimage.2009.09.033

Eichenbaum, H. (2017). Time (and space) in the hippocampus. *Current Opinion in Behavioral Sciences*, *17*, 65–70. https://doi.org/10.1016/j.cobeha.2017.06.010

Ekstrom, A. D., & Ranganath, C. (2018). Space, time, and episodic memory: The hippocampus is all over the cognitive map. *Hippocampus*, *28*(9), 680–687. https://doi.org/10.1002/hipo.22750

Gaffan, D. (1992). The role of the hippocampus-fornix-mammillary system in episodic memory. In L. R. Squire & N. Butters (Eds.), *Neuropsychology of memory* (pp. 336–346). Guilford Press.

Gaffan, D., & Hornak, J. (1997). Amnesia and neglect: Beyond the delay-Brion system and the Hebb synapse. *Philosophical Transactions of the Royal Society of London. Series B, Biological Sciences*, *352*(1360), 1481–1488. https://doi.org/10.1098/rstb.1997.0135

Gaffan, D., & Parker, A. (1996). Interaction of perirhinal cortex with the fornix-fimbria: Memory for objects and "object-in-place" memory. *The Journal of Neuroscience*, *16*(18), 5864–5869. https://doi.org/10.1523/jneurosci.16-18-05864.1996

Gagnon, A., Grenier, G., Bocti, C., Gillet, V., Lepage, J. F., Baccarelli, A. A., Posner, J., Descoteaux, M., & Takser, L. (2022). White matter microstructural variability linked to differential attentional skills and impulsive behavior in a pediatric population. *Cerebral Cortex*, bhac180. https://doi.org/10.1093/cercor/bhac180

Geeraert, B. L., Chamberland, M., Lebel, R. M., & Lebel, C. (2020). Multimodal principal component analysis to identify major features of white matter structure and links to reading. *PLoS ONE*, *15*(8), e0233244. https://doi.org/10.1371/journal.pone.0233244

Giacosa, C., Karpati, F. J., Foster, N. E., Penhune, V. B., & Hyde, K. L. (2016). Dance and music training have different effects on white matter diffusivity in sensorimotor pathways. *NeuroImage*, *135*, 273–286. https://doi.org/10.1016/j.neuroimage.2016.04.048

Gomez, J., Pestilli, F., Witthoft, N., Golarai, G., Liberman, A., Poltoratski, S., Yoon, J., & Grill-Spector, K. (2015). Functionally defined white matter reveals segregated pathways in human ventral temporal cortex associated with category-specific processing. *Neuron*, *85*(1), 216–227. https://doi.org/10.1016/j.neuron.2014.12.027

Graham, K. S., Barense, M. D., & Lee, A. C. (2010). Going beyond LTM in the MTL: A synthesis of neuropsychological and neuroimaging findings on the role of the medial temporal lobe in memory and perception. *Neuropsychologia*, *48*(4), 831–853. https://doi.org/10.1016/j.neuropsychologia.2010.01.001

Grotheer, M., Kubota, E., & Grill-Spector, K. (2022). Establishing the functional relevancy of white matter connections in the visual system and beyond. *Brain Structure & Function*, *227*(4), 1347–1356. https://doi.org/10.1007/s00429-021-02423-4

Guberman, G. I., Stojanovski, S., Nishat, E., Ptito, A., Bzdok, D., Wheeler, A. L., & Descoteaux, M. (2022). Multi-tract multi-symptom relationships in pediatric concussion. *eLife*, *11*, e70450. https://doi.org/10.7554/eLife.70450

Hanslmayr, S., & Staudigl, T. (2014). How brain oscillations form memories--a processing based perspective on oscillatory subsequent memory effects. *NeuroImage*, *85*(Pt 2), 648–655. https://doi.org/10.1016/j.neuroimage.2013.05.121

Herbet, G., Zemmoura, I., & Duffau, H. (2018). Functional anatomy of the inferior longitudinal fasciculus: From historical reports to current hypotheses. *Frontiers in Neuroanatomy*, *12*, 77. https://doi.org/10.3389/fnana.2018.00077

Herweg, N. A., Solomon, E. A., & Kahana, M. J. (2020). Theta oscillations in human memory. *Trends in Cognitive Sciences*, *24*(3), 208–227. https://doi.org/10.1016/j.tics.2019.12.006

Heuer, E., & Bachevalier, J. (2013). Working memory for temporal order is impaired after selective neonatal hippocampal lesions in adult rhesus macaques. *Behavioural Brain Research*, *239*, 55–62. https://doi.org/10.1016/j.bbr.2012.10.043

Hodgetts, C. J., Postans, M., Shine, J. P., Jones, D. K., Lawrence, A. D., & Graham, K. S. (2015). Dissociable roles of the inferior longitudinal fasciculus and fornix in face and place perception. *eLife*, *4*, e07902. https://doi.org/10.7554/eLife.07902

Hodgetts, C. J., Postans, M., Warne, N., Varnava, A., Lawrence, A. D., & Graham, K. S. (2017). Distinct contributions of the fornix and inferior longitudinal fasciculus to episodic and semantic autobiographical memory. *Cortex*, *94*, 1–14. https://doi.org/10.1016/j.cortex.2017.05.010

Hodgetts, C. J., Stefani, M., Williams, A. N., Kolarik, B. S., Yonelinas, A. P., Ekstrom, A. D., Lawrence, A. D., Zhang, J., & Graham, K. S. (2020). The role of the fornix in human navigational learning. *Cortex*, *124*, 97–110. https://doi.org/10.1016/j.cortex.2019.10.017

Hoffman, L. J., Ngo, C. T., Canada, K. L., Pasternak, O., Zhang, F., Riggins, T., & Olson, I. R. (2022). The fornix supports episodic memory during childhood. *Cerebral Cortex*, *32*, 5388–5403. https://doi.org/10.1093/cercor/bhac022

Hofstetter, S., Tavor, I., Tzur Moryosef, S., & Assaf, Y. (2013). Short-term learning induces white matter plasticity in the fornix. *The Journal of Neuroscience*, *33*(31), 12844–12850. https://doi.org/10.1523/jneurosci.4520-12.2013

Howard, M. W., & Eichenbaum, H. (2015). Time and space in the hippocampus. *Brain Research*, *1621*, 345–354. https://doi.org/10.1016/j.brainres.2014.10.069

Hsieh, L. T., Gruber, M. J., Jenkins, L. J., & Ranganath, C. (2014). Hippocampal activity patterns carry information about objects in temporal context. *Neuron*, *81*(5), 1165–1178. https://doi.org/10.1016/j.neuron.2014.01.015

Hsieh, L. T., & Ranganath, C. (2014). Frontal midline theta oscillations during working memory maintenance and episodic encoding and retrieval. *NeuroImage*, *85*, 721–729. https://doi.org/10.1016/j.neuroimage.2013.08.003

Huber, E., Henriques, R. N., Owen, J. P., Rokem, A., & Yeatman, J. D. (2019). Applying microstructural models to understand the role of white matter in cognitive development. *Developmental Cognitive Neuroscience*, *36*, 100624. https://doi.org/10.1016/j.dcn.2019.100624

Jankowski, M. M., Ronnqvist, K. C., Tsanov, M., Vann, S. D., Wright, N. F., Erichsen, J. T., Aggleton, J. P., & O'Mara, S. M. (2013). The anterior thalamus provides a subcortical circuit supporting memory and spatial navigation. *Frontiers in Systems Neuroscience*, *7*, 45. https://doi.org/10.3389/fnsys.2013.00045

JASP Team. (2021). JASP (Version 0.9.0.1) [computer software].

Jenkinson, M., Beckmann, C. F., Behrens, T. E., Woolrich, M. W., & Smith, S. M. (2012). FSL. *NeuroImage*,

62(2), 782–790. https://doi.org/10.1016/j.neuroimage.2011.09.015

Jones, D. K., Christiansen, K. F., Chapman, R. J., & Aggleton, J. P. (2013). Distinct subdivisions of the cingulum bundle revealed by diffusion MRI fibre tracking: Implications for neuropsychological investigations. *Neuropsychologia*, *51*(1), 67–78. https://doi.org/10.1016/j.neuropsychologia.2012.11.018

Jones, D. K., Knosche, T. R., & Turner, R. (2013). White matter integrity, fiber count, and other fallacies: The do's and don'ts of diffusion MRI. *NeuroImage*, *73*, 239–254. https://doi.org/10.1016/j.neuroimage.2012.06.081

Kalm, K., Davis, M. H., & Norris, D. (2013). Individual sequence representations in the medial temporal lobe. *Journal of Cognitive Neuroscience*, *25*(7), 1111–1121. https://doi.org/10.1162/jocn_a_00378

Karahan, E., Costigan, A. G., Graham, K. S., Lawrence, A. D., & Zhang, J. (2019). Cognitive and white-matter compartment models reveal selective relations between corticospinal tract microstructure and simple reaction time. *The Journal of Neuroscience*, *39*(30), 5910–5921. https://doi.org/10.1523/jneurosci.2954-18.2019

Kassambara, A. (2019). ggcorrplot: Visualization of a correlation matrix using 'ggplot2'.

Kaufmann, L. K., Baur, V., Hänggi, J., Jäncke, L., Piccirelli, M., Kollias, S., Schnyder, U., Pasternak, O., Martin-Soelch, C., & Milos, G. (2017). Fornix under water? Ventricular enlargement biases forniceal diffusion magnetic resonance imaging indices in anorexia nervosa. *Biol Psychiatry Cogn Neurosci Neuroimaging*, *2*(5), 430–437. https://doi.org/10.1016/j.bpsc.2017.03.014

Kirk, I. J. (1998). Frequency modulation of hippocampal theta by the supramammillary nucleus, and other hypothalamo-hippocampal interactions: Mechanisms and functional implications. *Neuroscience and Biobehavioral Reviews*, *22*(2), 291–302. https://doi.org/10.1016/s0149-7634(97)00015-8

Latini, F., Mårtensson, J., Larsson, E. M., Fredrikson, M., Åhs, F., Hjortberg, M., Aldskogius, H., & Ryttlefors, M. (2017). Segmentation of the inferior longitudinal fasciculus in the human brain: A white matter dissection and diffusion tensor tractography study. *Brain Research*, *1675*, 102–115. https://doi.org/10.1016/j.brainres.2017.09.005

Leao, R. N., Targino, Z. H., Colom, L. V., & Fisahn, A. (2015). Interconnection and synchronization of neuronal populations in the mouse medial septum/diagonal band of Broca. *Journal of Neurophysiology*, *113*(3), 971–980. https://doi.org/10.1152/jn.00367.2014

Lee, A. C. H., Thavabalasingam, S., Alushaj, D., Çavdaroğlu, B., & Ito, R. (2020). The hippocampus contributes to temporal duration memory in the context of event sequences: A cross-species perspective. *Neuropsychologia*, *137*, 107300. https://doi.org/10.1016/j.neuropsychologia.2019.107300

Leemans, A., Jeurissen, B., Sijbers, J., & Jones, D. K. (2009). ExploreDTI: a graphical toolbox for processing, analyzing, and visualizing diffusion MR data. In: 17th Annual Meeting of Intl Soc Mag Reson Med, (p. 3537). Hawaii, USA.

Liang, M., Zheng, J., Isham, E., & Ekstrom, A. (2021). Common and distinct roles of frontal midline theta and occipital alpha oscillations in coding temporal intervals and spatial distances. *Journal of Cognitive Neuroscience*, *33*(11), 2311–2327. https://doi.org/10.1162/jocn_a_01765

Lisman, J., & Redish, A. D. (2009). Prediction, sequences and the hippocampus. *Philosophical Transactions of the Royal Society of London. Series B, Biological Sciences*, *364*(1521), 1193–1201. https://doi.org/10.1098/rstb.2008.0316

Long, N. M., & Kahana, M. J. (2019). Hippocampal contributions to serial-order memory. *Hippocampus*, *29*(3), 252–259. https://doi.org/10.1002/hipo.23025

Luo, Z., Adluru, N., Dean, D. C. 3rd, Alexander, A. L., & Goldsmith, H. H. (2022). Genetic and environmental influences of variation in diffusion MRI measures of white matter microstructure. *Brain Structure & Function*, *227*(1), 131–144. https://doi.org/10.1007/s00429-021-02393-7

Mathiasen, M. L., Louch, R. C., Nelson, A. D., Dillingham, C. M., & Aggleton, J. P. (2019). Trajectory of hippocampal fibres to the contralateral anterior thalamus and mammillary bodies in rats, mice, and macaque monkeys. *Brain Neurosci Adv*, *3*, 2398212819871205. https://doi.org/10.1177/2398212819871205

MATLAB. (2015). MATLAB version 8.5.0.197613 (R2015a). In The MathWorks Inc.

McDonald, J. H. (2014). *Handbook of biological statistics* (3rd ed.). Sparky House Publishing.

McNab, J. A., Edlow, B. L., Witzel, T., Huang, S. Y., Bhat, H., Heberlein, K., Feiweier, T., Liu, K., Keil, B., Cohen-Adad, J., Tisdall, M. D., Folkerth, R. D., Kinney, H. C., & Wald, L. L. (2013). The human connectome project and beyond: Initial applications of 300 mT/m gradients. *NeuroImage*, *80*, 234–245. https://doi.org/10.1016/j.neuroimage.2013.05.074

McNaughton, N., Ruan, M., & Woodnorth, M. A. (2006). Restoring theta-like rhythmicity in rats restores initial learning in the Morris water maze. *Hippocampus*, *16*(12), 1102–1110. https://doi.org/10.1002/hipo.20235

Mollink, J., Kleinnijenhuis, M., Cappellen van Walsum, A. V., Sotiropoulos, S. N., Cottaar, M., Mirfin, C., Heinrich, M. P., Jenkinson, M., Pallebage-Gamarallage, M., Ansorge, O., Jbabdi, S., & Miller, K. L. (2017). Evaluating fibre orientation dispersion in white matter: Comparison of diffusion MRI, histology and polarized light imaging. *NeuroImage*, *157*, 561–574. https://doi.org/10.1016/j.neuroimage.2017.06.001

Morey, M. D., & Rouder, J. N. (2018). BayesFactor: Computation of Bayes factors for common designs. R package version 0.9.12–4.3. CRAN.R-project.org/package=BayesFactor

Murray, E. A., Wise, S. P., & Graham, K. S. (2017). *The evolution of memory systems: Ancestors, anatomy, and adaptations*. Oxford University Press.

Murray, E. A., Wise, S. P., & Graham, K. S. (2018). Representational specializations of the hippocampus in phylogenetic perspective. *Neuroscience Letters*, *680*, 4–12. https://doi.org/10.1016/j.neulet.2017.04.065

Nelson, A. J. D. (2021). The anterior thalamic nuclei and cognition: A role beyond space? *Neuroscience and Biobehavioral Reviews*, *126*, 1–11. https://doi.org/10.1016/j.neubiorev.2021.02.047

Opitz, B. (2014). Memory function and the hippocampus. *Frontiers of Neurology and Neuroscience*, *34*, 51–59. https://doi.org/10.1159/000356422

Pan, W. X., & McNaughton, N. (2004). The supramammillary area: Its organization, functions and relationship to the hippocampus. *Progress in Neurobiology*, *74*(3), 127–166. https://doi.org/10.1016/j.pneurobio.2004.09.003

Panesar, S. S., Yeh, F.-C., Jacquesson, T., Hula, W., & Fernandez-Miranda, J. C. (2018). A quantitative tractography study into the connectivity, segmentation and laterality of the human inferior longitudinal fasciculus. *Frontiers in Neuroanatomy*, *12*, 47. https://doi.org/10.3389/fnana.2018.00047

Parker, A., & Gaffan, D. (1997). The effect of anterior thalamic and cingulate cortex lesions on object-in-place memory in monkeys. *Neuropsychologia*, *35*(8), 1093–1102. https://doi.org/10.1016/s0028-3932(97)00042-0

Parker, G., Marshall, D., Rosin, P. L., Drage, N., Richmond, S., & Jones, D. (2012). RESDORE: Robust estimation in spherical deconvolution by outlier rejection. URL: archive.ismrm.org/2013/3148.html

Pasternak, O., Sochen, N., Gur, Y., Intrator, N., & Assaf, Y. (2009). Free water elimination and mapping from diffusion MRI. *Magnetic Resonance in Medicine*, *62*(3), 717–730. https://doi.org/10.1002/mrm.22055

Patil, I. (2021). Visualizations with statistical details: The 'ggstatsplot' approach. *Journal of Open Source Software*, *6*(61), 3167. https://doi.org/10.21105/joss.03167

Pierpaoli, C., Jezzard, P., Basser, P. J., Barnett, A., & di Chiro, G. (1996). Diffusion tensor MR imaging of the human brain. *Radiology*, *201*(3), 637–648. https://doi.org/10.1148/radiology.201.3.8939209

Pines, A. R., Cieslak, M., Larsen, B., Baum, G. L., Cook, P. A., Adebimpe, A., Dávila, D. G., Elliott, M. A., Jirsaraie, R., Murtha, K., Oathes, D. J., Piiwaa, K., Rosen, A. F. G., Rush, S., Shinohara, R. T., Bassett, D. S., Roalf, D. R., & Satterthwaite, T. D. (2020). Leveraging multi-shell diffusion for studies of brain development in youth and young adulthood. *Developmental Cognitive Neuroscience*, *43*, 100788. https://doi.org/10.1016/j.dcn.2020.100788

Poletti, C. E., & Creswell, G. (1977). Fornix system efferent projections in the squirrel monkey: An experimental degeneration study. *The Journal of Comparative Neurology*, *175*(1), 101–128. https://doi.org/10.1002/cne.901750107

Postans, M., Hodgetts, C. J., Mundy, M. E., Jones, D. K., Lawrence, A. D., & Graham, K. S. (2014). Interindividual variation in fornix microstructure and macrostructure is related to visual discrimination accuracy for scenes but not faces. *The Journal of Neuroscience*, *34*(36), 12121–12126. https://doi.org/10.1523/jneurosci.0026-14.2014

Pu, Y., Cheyne, D. O., Cornwell, B. R., & Johnson, B. W. (2018). Non-invasive investigation of human hippocampal rhythms using magnetoencephalography: A review. *Frontiers in Neuroscience*, *12*, 273. https://doi.org/10.3389/fnins.2018.00273

R Core Team. (2019). R: A language and environment for statistical computing. (Available at: R-project.org/). Vienna, Austria: R Foundation for Statistical Computing.

Radwan, A. M., Sunaert, S., Schilling, K., Descoteaux, M., Landman, B. A., Vandenbulcke, M., Theys, T., Dupont, P., & Emsell, L. (2022). An atlas of white matter anatomy, its variability, and reproducibility based on constrained spherical deconvolution of diffusion MRI. *NeuroImage*, *254*, 119029. https://doi.org/10.1016/j.neuroimage.2022.119029

Raftery, A. E. (1995). Bayesian model selection in social research. *Sociological Methodology*, *25*, 111–163. https://doi.org/10.2307/271063

Ranganath, C. (2010). A unified framework for the functional organization of the medial temporal lobes and the phenomenology of episodic memory. *Hippocampus*, *20*(11), 1263–1290. https://doi.org/10.1002/hipo.20852

Ranganath, C., & Hsieh, L.-T. (2016). The hippocampus: A special place for time. *Annals of the new York Academy of Sciences*, *1369*(1), 93–110. https://doi.org/10.1111/nyas.13043

Rawlins, J. N., Feldon, J., & Gray, J. A. (1979). Septo-hippocampal connections and the hippocampal theta rhythm. *Experimental Brain Research*, *37*(1), 49–63. https://doi.org/10.1007/bf01474253

Reddy, L., Self, M. W., Zoefel, B., Poncet, M., Possel, J. K., Peters, J. C., Baayen, J. C., Idema, S., VanRullen, R., & Roelfsema, P. R. (2021). Theta-phase dependent neuronal coding during sequence learning in human single neurons. *Nature Communications*, *12*(1), 4839. https://doi.org/10.1038/s41467-021-25150-0

Revelle, W. (2022). psych: Procedures for personality and psychological research, Northwestern University, Evanston, Illinois, USA. CRAN.R-project.org/package=psych Version = 2.2.3.

RStudio Team. (2020). RStudio: Integrated development for R. RStudio, PBC, Boston, MA URL http://www.rstudio.com/

Rudebeck, S. R., Scholz, J., Millington, R., Rohenkohl, G., Johansen-Berg, H., & Lee, A. C. (2009). Fornix microstructure correlates with recollection but not familiarity memory. *The Journal of Neuroscience*, *29*(47), 14987–14992. https://doi.org/10.1523/jneurosci.4707-09.2009

Sato, K., Kerever, A., Kamagata, K., Tsuruta, K., Irie, R., Tagawa, K., Aoki, S., Arikawa-Hirasawa, E., Nitta, N., & Aoki, I. (2017). Understanding microstructure of the brain by comparison of neurite orientation dispersion and density imaging (NODDI) with transparent mouse brain. *Acta Radiologica Open*, *6*(4), 2058460117703816. https://doi.org/10.1177/2058460117703816

Saunders, R. C., & Aggleton, J. P. (2007). Origin and topography of fibers contributing to the fornix in macaque monkeys. *Hippocampus*, *17*(5), 396–411. https://doi.org/10.1002/hipo.20276

Saunders, R. C., Mishkin, M., & Aggleton, J. P. (2005). Projections from the entorhinal cortex, perirhinal cortex, presubiculum, and parasubiculum to the medial thalamus in macaque monkeys: Identifying different pathways using disconnection techniques. *Experimental Brain Research*, *167*(1), 1–16. https://doi.org/10.1007/s00221-005-2361-3

Schapiro, A. C., Kustner, L. V., & Turk-Browne, N. B. (2012). Shaping of object representations in the human medial temporal lobe based on temporal regularities. *Current Biology*, *22*(17), 1622–1627. https://doi.org/10.1016/j.cub.2012.06.056

Schapiro, A. C., Turk-Browne, N. B., Norman, K. A., & Botvinick, M. M. (2016). Statistical learning of temporal community structure in the hippocampus. *Hippocampus*, *26*(1), 3–8. https://doi.org/10.1002/hipo.22523

Schilling, K. G., Janve, V., Gao, Y., Stepniewska, I., Landman, B. A., & Anderson, A. W. (2018). Histological validation of diffusion MRI fiber orientation distributions and dispersion. *NeuroImage*, *165*, 200–221. https://doi.org/10.1016/j.neuroimage.2017.10.046

Schilling, K. G., Petit, L., Rheault, F., Remedios, S., Pierpaoli, C., Anderson, A. W., Landman, B. A., & Descoteaux, M. (2020). Brain connections derived from diffusion MRI tractography can be highly anatomically accurate-if we know where white

matter pathways start, where they end, and where they do not go. *Brain Structure & Function*, *225*(8), 2387–2402. https://doi.org/10.1007/s00429-020-02129-z

Seehaus, A., Roebroeck, A., Bastiani, M., Fonseca, L., Bratzke, H., Lori, N., Vilanova, A., Goebel, R., & Galuske, R. (2015). Histological validation of high-resolution DTI in human post mortem tissue. *Frontiers in Neuroanatomy*, *9*, 98. https://doi.org/10.3389/fnana.2015.00098

Sibilia, F., Kehoe, E. G., Farrell, D., Kerskens, C., O'Neill, D., McNulty, J. P., Mullins, P., & Bokde, A. L. W. (2017). Aging-related microstructural alterations along the length of the cingulum bundle. *Brain Connectivity*, *7*(6), 366–372. https://doi.org/10.1089/brain.2017.0493

Skaggs, W. E., McNaughton, B. L., Wilson, M. A., & Barnes, C. A. (1996). Theta phase precession in hippocampal neuronal populations and the compression of temporal sequences. *Hippocampus*, *6*(2), 149–172. 10.1002/(sici)1098-1063(1996)6:2<149::aid-hipo6>3.0.co;2-k

Smith, S. M. (2002). Fast robust automated brain extraction. *Human Brain Mapping*, *17*(3), 143–155. https://doi.org/10.1002/hbm.10062

Solomon, E. A., Kragel, J. E., Gross, R., Lega, B., Sperling, M. R., Worrell, G., Sheth, S. A., Zaghloul, K. A., Jobst, B. C., Stein, J. M., Das, S., Gorniak, R., Inman, C. S., Seger, S., Rizzuto, D. S., & Kahana, M. J. (2018). Medial temporal lobe functional connectivity predicts stimulation-induced theta power. *Nature Communications*, *9*(1), 4437. https://doi.org/10.1038/s41467-018-06876-w

Solomon, E. A., Stein, J. M., Das, S., Gorniak, R., Sperling, M. R., Worrell, G., Inman, C. S., Tan, R. J., Jobst, B. C., Rizzuto, D. S., & Kahana, M. J. (2019). Dynamic theta networks in the human medial temporal lobe support episodic memory. *Current Biology*, *29*, 1100–1111.e4. https://doi.org/10.1016/j.cub.2019.02.020

Swanson, L. W., & Cowan, W. M. (1979). The connections of the septal region in the rat. *The Journal of Comparative Neurology*, *186*(4), 621–655. https://doi.org/10.1002/cne.901860408

Tavor, I., Yablonski, M., Mezer, A., Rom, S., Assaf, Y., & Yovel, G. (2014). Separate parts of occipito-temporal white matter fibers are associated with recognition of faces and places. *NeuroImage*, *86*, 123–130. https://doi.org/10.1016/j.neuroimage.2013.07.085

Tournier, J. D., Mori, S., & Leemans, A. (2011). Diffusion tensor imaging and beyond. *Magnetic Resonance in Medicine*, *65*(6), 1532–1556. https://doi.org/10.1002/mrm.22924

Tsanov, M., Wright, N., Vann, S. D., Erichsen, J. T., Aggleton, J. P., & O'Mara, S. M. (2011). Hippocampal inputs mediate theta-related plasticity in anterior thalamus. *Neuroscience*, *187*, 52–62. https://doi.org/10.1016/j.neuroscience.2011.03.055

Tuch, D. S., Reese, T. G., Wiegell, M. R., Makris, N., Belliveau, J. W., & Wedeen, V. J. (2002). High angular resolution diffusion imaging reveals intravoxel white matter fiber heterogeneity. *Magnetic Resonance in Medicine*, *48*(4), 577–582. https://doi.org/10.1002/mrm.10268

Vaher, K., Galdi, P., Blesa Cabez, M., Sullivan, G., Stoye, D. Q., Quigley, A. J., Thrippleton, M. J., Bogaert, D., Bastin, M. E., Cox, S. R., & Boardman, J. P. (2022). General factors of white matter microstructure from DTI and NODDI in the developing brain. *NeuroImage*, *254*, 119169. https://doi.org/10.1016/j.neuroimage.2022.119169

Wakana, S., Caprihan, A., Panzenboeck, M. M., Fallon, J. H., Perry, M., Gollub, R. L., Hua, K., Zhang, J., Jiang, H., Dubey, P., Blitz, A., van Zijl, P., & Mori, S. (2007). Reproducibility of quantitative tractography methods applied to cerebral white matter. *NeuroImage*, *36*(3), 630–644. https://doi.org/10.1016/j.neuroimage.2007.02.049

Wickham, H. (2016). *ggplot2: Elegant graphics for data analysis*. Springer-Verlag New York. https://doi.org/10.1007/978-3-319-24277-4

Williams, A. B., Liu, X., Hsieh, F., Hurtado, M., Lesh, T., Niendam, T., Carter, C., Ranganath, C., & Ragland, J. D. (2023). Memory-based prediction deficits and dorsolateral prefrontal dysfunction in schizophrenia. *Biological Psychiatry: Cognitive Neuroscience and Neuroimaging*, *8*(1), 71–78. https://doi.org/10.1016/j.bpsc.2022.05.006

Żakowski, W., Zawistowski, P., Braszka, Ł., & Jurkowlaniec, E. (2017). The effect of pharmacological inactivation of the mammillary body and anterior thalamic nuclei on hippocampal theta rhythm in urethane-anesthetized rats. *Neuroscience*, *362*, 196–205. https://doi.org/10.1016/j.neuroscience.2017.08.043

Zhang, H., Schneider, T., Wheeler-Kingshott, C. A., & Alexander, D. C. (2012). NODDI: Practical in vivo neurite orientation dispersion and density imaging of the human brain. *NeuroImage*, *61*(4), 1000–1016. https://doi.org/10.1016/j.neuroimage.2012.03.072

SUPPORTING INFORMATION

Additional supporting information can be found online in the Supporting Information section at the end of this article.

How to cite this article: Read, M.-L., Umla-Runge, K., Lawrence, A. D., Costigan, A. G., Hsieh, L.-T., Chamberland, M., Ranganath, C., & Graham, K. S. (2023). A role for the fornix in temporal sequence memory. *European Journal of Neuroscience*, *57*(7), 1141–1160. https://doi.org/10.1111/ejn.15940